

Nonlinear dissipation phenomena in optomechanics

Master's thesis

December 7, 2016

Author:

JUUSO MANNINEN

Instructor:

FRANCESCO MASSEL



UNIVERSITY OF JYVÄSKYLÄ
DEPARTMENT OF PHYSICS

Abstract

Author: Juuso Manninen

Title: Nonlinear dissipation phenomena in optomechanics

Date: December 7, 2016

Language: English

5 + 59 pages

University of Jyväskylä
Faculty of Mathematics and Science
Department of Physics

Instructor: Francesco Massel

A quantum system cannot be completely isolated from its environment, meaning that information is transmitted between them.

In optomechanics, where a typical system under study is an optical cavity consisting of highly reflective mirrors coupled with a mechanical resonator, dissipation phenomena related to linear system-environment coupling are well known. However, nonlinear phenomena are not understood to the same extent.

I consider a nonlinear coupling between a cavity and a heat bath, and illustrate the effects of this coupling such as nonlinear dissipation of the cavity. I also propose a model, where an optical cavity and a heat bath interact with two-level systems, justifying nonlinear dissipation for the optical cavity.

To give some context to the results of this work, I include introductory reviews of optomechanics, open quantum systems, and two-level systems together with the methods used to study these topics. I also provide some calculations of simplified setups as well as full derivations of the methods used in this work for a more pedagogical approach.

Keywords: optomechanics, open quantum systems, nonlinear dissipation, input-output formalism, Master equation, Schrieffer–Wolff transformation

Tiivistelmä

Tekijä: Juuso Manninen

Otsikko: Epälineaariset dissipaatioilmiöt optomekaniikassa

Päivämäärä: 7. joulukuuta 2016

Kieli: englanti

5 + 59 sivua

Jyväskylän yliopisto
Matemaattis-luonnontieteellinen tiedekunta
Fysiikan laitos

Ohjaaja: Francesco Massel

Yksikään kvanttisysteemi ei voi olla täysin eristetty ympäristöstään, mikä johtaa informaation välittämiseen systeemin ja ympäristön välillä.

Optomekaniikassa, missä tyypillinen tutkittava systeemi on peileistä koostuva optinen kaviteetti yhdistettynä mekaaniseen värähtelijään, systeemin ja ympäristön lineaarisesta kytkennästä johtuvat dissipaatioilmiöt ovat hyvin tunnettuja. Epälineaarisia ilmiöitä ei kuitenkaan ymmärretä yhtä laajasti.

Tutkin epälineaarista kytkentää kaviteetin ja lämpökylvyn välillä ja havainnollistan tästä kytkennästä johtuvia ilmiöitä kuten epälineaarista dissipaatiota. Esitän myös optisen kaviteetin epälineaarisen dissipaation oikeuttavan mallin, missä optinen kaviteetti ja lämpökylpy vuorovaikuttavat kaksitilasysteemien kanssa.

Antaakseni tämän työn tuloksille kontekstia, sisällytän pohjustavat katsaukset optomekaniikkaan, avoimiin kvanttisysteemeihin ja kaksitilasysteemeihin sekä näiden aihealueiden tutkimiseen käytettäviin menetelmiin. Esitän myös esimerkkilaskuja yksinkertaistetuista malleista ja lisäksi johdan kaikki tässä työssä käytetyt menetelmät mahdollisimman pedagogisen lähesymistävän saavuttamiseksi.

Avainsanat: optomekaniikka, avoimet kvanttisysteemit, epälineaarinen dissipaatio, siirräntäformalisismi, Master-yhtälö, Schrieffer–Wolff –muunnos

Contents

1	Introduction	1
2	Review of optomechanics	3
2.1	Cavity and mechanical motion	3
2.2	Optomechanical system	6
3	Open quantum systems	8
3.1	The Markov process	8
3.2	Input-output formalism	10
3.3	Linear formulation of optomechanics	13
3.4	Master equation approach	17
4	Nonlinear model Hamiltonian	23
4.1	Derivation of the quantum Langevin equation	24
4.2	Solving the nonlinear quantum Langevin equation	25
4.3	Master equation for the nonlinearly dissipative harmonic oscillator	31
5	Review of two-level systems	34
5.1	Algebra of two-level systems	34
5.2	Modeling two-level systems and the interaction with them	35
6	Derivation of nonlinear phenomena	38
6.1	Interaction between light and matter	38
6.2	Schrieffer–Wolff transformation	43
7	Conclusions	48
	References	49
A	Derivation of the QLE for the nonlinear model Hamiltonian	53
B	Derivation of the metastable–stable threshold value	55
C	Derivation of the Schrieffer–Wolff transformation	57
D	Fourier transform conventions	59

Introduction

One of the first scientific speculations about light affecting the motion of a mechanical object was made by Kepler [1] as early as in 1619 on the basis of his observations that the tails of comets seemed to point away from the sun as they passed it by. The idea that light could carry momentum was expanded a century later as Newton proposed the first particle theory of light based on his measurements of refraction and reflection of light [2]. Maxwell advanced the study of light considerably by formulating mathematically the behaviour of electromagnetic radiation [3]. Later Einstein discussed that the momentum carried by photons, particles of light, causes a *radiation pressure* on a surface that is exposed to light [4]. While the pressure force is far too weak to be encountered in our daily lives, e.g. you do not feel the recoil of a flashlight when you turn it on, the effect is still measurable as shown by Nichols and Hull [5], using a delicate torsion system, as well as by Lebedev [6] in the early 20th century. In 1978 Ashkin proposed a method of trapping single atoms using the radiation pressure force [7] later known as optical tweezing. Another application of radiation pressure, laser cooling of atoms that takes advantage of the Doppler shift of lasers pointed at atoms from different directions, was introduced also in the 1970's, e.g. by Hänsch and Schawlow [8]. Other cooling techniques, including methods using *optical cavities*, related to cold atoms are discussed by Chu in his review [9]. The progress in laser interferometry lead to the very recent direct observation of gravitational waves [10]. A more extensive and detailed look on the development of the field of *optomechanics*, the study of light-matter coupling, is provided by Aspelmeyer et al. [11].

Even though optomechanics emerged as a research field over the last few decades, a lot of advancement has been made in such a short time. There are a few astonishing phenomena arising from the radiation pressure that electromagnetic radiation exerts on mechanical apparatuses. The ability to observe and manipulate nonclassical behaviour of mechanical motion [12] revealing completely new kinds of classically impossible states using light is one of the main motivations driving the study of optomechanical field of physics forward. Similarly one can use optomechanical setups e.g. to measure extremely small displacements [13], or to test fundamental aspects of quantum mechanics like decoherence in macroscopic objects [11] with the help of quantum mechanical adjustments of ever larger systems. One other possible application of an optomechanical setup is its usage as a memory element in quantum computing [14].

Since a quantum system cannot be completely isolated from its environment in reality, in order to properly model the time evolution of the system, the effects of the environment on the system need to be considered as well. There are many possible approaches for studying open quantum systems and they are used in various research fields of physics. In this work, I concentrate on the input-output formalism as well as the Master equation approach because of their applicability in optomechanics. Other examples of techniques used in the field of open quantum systems are represented by non-equilibrium Green's

functions which are used to study transport phenomena in mesoscopic systems [15], and the LSZ reduction which is utilized in scattering problems in particle physics [16], but these two methods are not within the scope of this thesis.

The remark that the quantum system is open leads to the notion of *dissipation*, the ability of the system to lose energy to the environment that it is interacting with or to transform it to some unusable form. In general, dissipation can be considered as irreversible energy loss from the system to the environment degrees of freedom [17]. Note that irreversible processes increase the entropy of the system [18]. One example of this is friction that turns a part of the energy corresponding to some mechanical motion into heat that dissipates into the environment. Thus the dissipated energy is effectively lost since it can no longer be accessed by the system. Additionally, an open quantum system is subject to *decoherence*, the loss of quantum superposition states into classical ones. This is the underlying reason for the classical behaviour of macroscopic objects [19].

There are several dissipation mechanisms in optomechanical systems, e.g. the damping of studied mechanical motion due to friction, photons escaping from an optical cavity due to the mirrors not being perfect, and resistance in electric circuits in the context of circuit optomechanics, just to name a few. For simple systems linear dissipation models are enough to explain their behaviour. However, the advances in material technology have made the construction of micro and nano scale resonators possible, and nonlinear damping has been measured e.g. in carbon nanotube and graphene resonators [20]. What is meant by linear and nonlinear dissipation becomes apparent in this work.

Chapter 2 introduces the basic concepts of optomechanics followed by Chap. 3 detailing open quantum systems. In Chap. 4, I construct a nonlinear model Hamiltonian, depicting a cavity, a heat bath environment, and their mutual interaction, to demonstrate the effects that a nonlinear system-environment coupling has on the time evolution of cavity field operators. Chapter 5 serves as an introduction to two-level systems to work as a background for Chap. 6 that focuses on showing how nonlinearities can arise from two-level systems interacting with an optical cavity and its environment using quantum electrodynamics (QED) and Schrieffer-Wolff formalism.

Review of optomechanics

In this Chapter, I review the basics of optomechanics to familiarize the reader with the research field and to motivate the results provided in this thesis. Although, in this work, I do not discuss the physics of the optomechanical coupling, but I solely focus on the dissipative properties of the cavity and the mechanical oscillator, this Chapter is constructed to provide the reader with enough context to understand how the main results of this thesis are related to optomechanics in general.

As one might expect, optomechanics involves both optical and mechanical aspects. In Sec. 2.1, I introduce these concepts separately and then combine them in Sec. 2.2 to form a complete picture of a full optomechanical system.

2.1 Cavity and mechanical motion

An optical cavity is a setup of mirrors that is able to reflect light so that it forms standing waves, designated as modes, inside the cavity, see Fig. 1. Each of these modes has a characteristic frequency, unique to it. The simplest type of optical cavity is the Fabry-Pérot cavity that consists of two flat reflective surfaces facing each other where one mirror is semi-transparent so that a laser beam can be directed into the cavity. It is easy to see that, for a standing electromagnetic (EM) wave to form inside such a setup, its angular frequency is required to be

$$\omega_{\text{cav},n} = \frac{n\pi c}{L}, \quad (2.1)$$

where $n \in \mathbb{N}$ is the mode number, c the speed of light, and L the separation of the two mirrors. In this work, I only focus on cavities and mechanical oscillators whose modes are spaced so sparsely that one is allowed to consider a single mode denoted by ω_{cav} for the cavity and ω_{m} for the mechanics. This is a fairly accurate assumption for an optical cavity whose lengths typically range from 10^{-5} m to 10^{-2} m [11], since these lengths correspond to mode separations of the orders 10^{10} Hz to 10^{13} Hz.

Even though the mirrors of the cavity are very highly reflecting, they are not perfect and some photons are lost from the cavity. A useful quantity for defining the reflectiveness of the cavity is the quality factor

$$Q_{\text{opt}} = \omega_{\text{cav}}\tau = 2\pi \frac{\tau}{T_{\text{cav}}}, \quad (2.2)$$

where τ is the lifetime of a photon inside the cavity and T_{cav} is the period of the fundamental mode. Because of the τ/T_{cav} dependence, the quality factor can be tied to the number of times an average photon can make the trip back and forth in the cavity. τ can be written as the inverse of the damping rate of the cavity, κ . The damping can arise from both internal properties of the cavity and external influences, e.g. the coupling between

the cavity and the environment. For a Fabry-Pérot cavity the obvious loss mechanism is that the mirrors are not perfectly reflective. This is emphasized by the fact that the other mirror is semi-transparent so that the light can be directed into the cavity in the first place. [11]

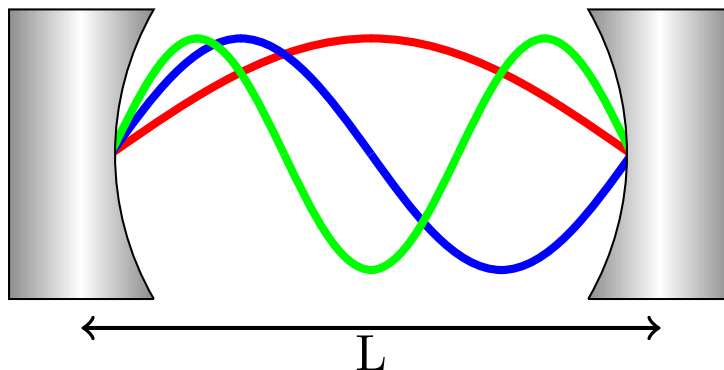


Figure 1: Standing waves form as the result of the interference of two waves, the left and right moving electromagnetic fields in this case, and they are defined by their boundary conditions so that there are nodes at both ends of the cavity. This schematic shows the three modes with the smallest frequencies, the fundamental mode (red), the second (blue), and the third mode (green).

An optical cavity with stationary mirrors can be modeled with a quantum mechanical Hamiltonian of a harmonic oscillator with a fundamental mode ω_{ho}

$$H_{\text{ho}} = \omega_{\text{ho}} O^\dagger O + \frac{\omega_{\text{ho}}}{2}, \quad (2.3)$$

where $O^{(\dagger)}$ is the second quantized annihilation (creation) field operator of the harmonic oscillator.

Despite its very different appearance compared to a cavity, also a simple mechanical resonator can be described by a similar Hamiltonian in the context of quantum mechanics. Classically linear theory of elasticity can be applied to solve the vibrational modes of the mechanical oscillator provided that its geometry is known [21]. With proper normalization a classical equation of motion (EOM) [11]

$$m_{\text{eff}} \frac{d^2 x(t)}{dt^2} + m_{\text{eff}} \gamma_m \frac{dx(t)}{dt} + m_{\text{eff}} \omega_m^2 x(t) = F_{\text{ext}}(t) \quad (2.4)$$

of a harmonic oscillator with a single mechanical angular frequency ω_m is obtained. Focusing solely on one mechanical frequency requires the assumption that the mechanical modes are sparsely distributed, similarly to the modes of the cavity mentioned above. Here m_{eff} is the effective mass of the oscillator, $x(t)$ the time-dependent displacement, γ_m the mechanical damping rate, and $F_{\text{ext}}(t)$ the net external force. The external forces can include e.g. mechanical driving or the stochastic thermal motion caused by the environment of the resonator. Similar to the optical case Eq. (2.2), the quality factor of a mechanical oscillator is defined

$$Q_{\text{mec}} = \frac{\omega_m}{\gamma_m}. \quad (2.5)$$

It is worth noticing that the effective mass of the mechanical oscillator is not always its physical mass. For simple oscillating systems, e.g. an uncoupled harmonic oscillator, the

displacement $x(t)$ is naturally defined as the displacement of the center of mass which leads the effective mass being the physical mass. However, for some systems the definition of the displacement coordinate is not as clear, and this can deviate the effective mass from the physical mass. Effective mass can, however, always be determined using the linear theory of elasticity, and comparing the effective mass given by that theory to the requirement that the potential energy of the oscillator is of the form $U = m_{\text{eff}}\omega_m^2\langle x^2(t)\rangle/2$.

Using the Fourier transform convention $x(\omega) = \int dt e^{i\omega t}x(t)$, the classical EOM (2.4) can be solved to yield

$$x(\omega) = \chi_m(\omega) F_{\text{ext}}(\omega), \quad (2.6)$$

where $\chi_m(\omega) = [m_{\text{eff}}(\omega_m^2 - \omega^2) - im_{\text{eff}}\gamma_m\omega]^{-1}$ is the susceptibility of the mechanical resonator. This solution shows explicitly how the mechanical motion is affected by the external force, i.e. the response of the mechanics. Figure 2 shows schematically how changing different parameter values affects the response of the mechanical oscillator.

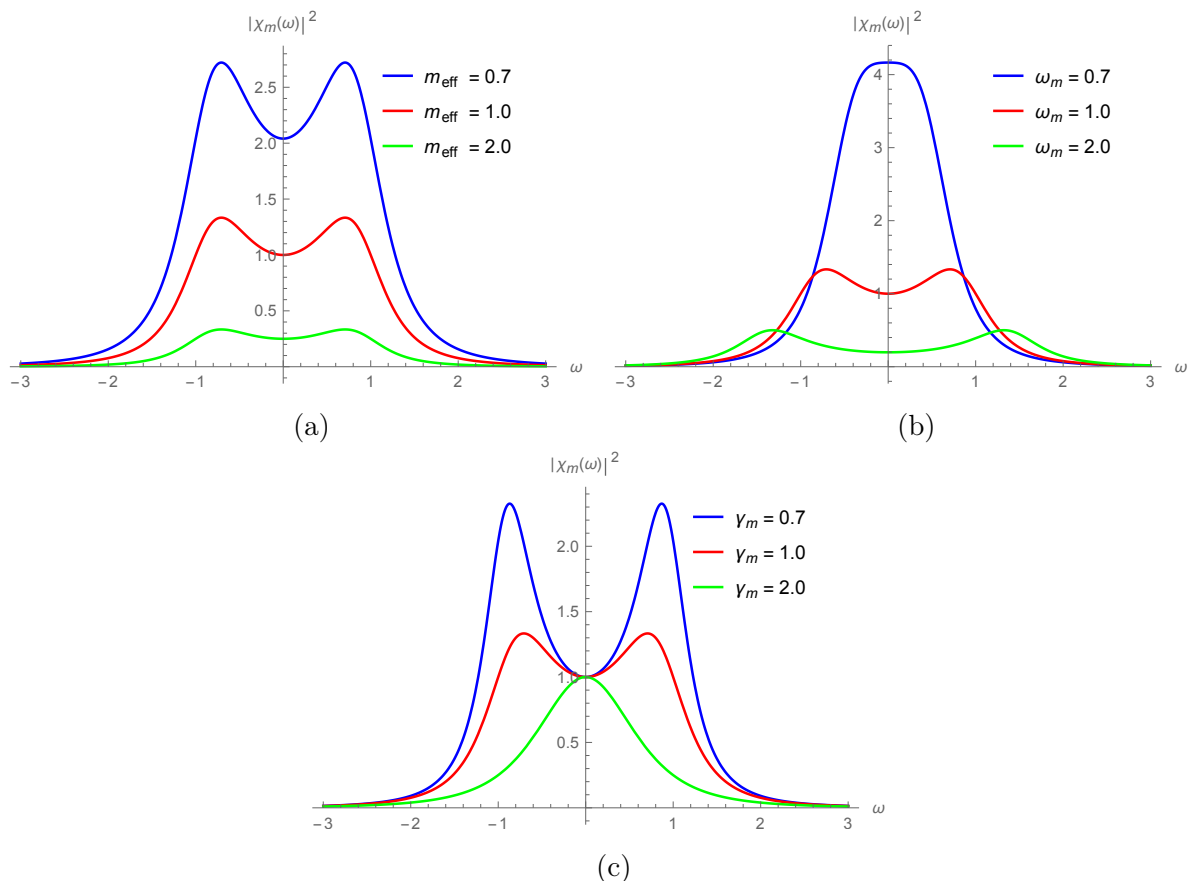


Figure 2: The response of a mechanical oscillator to an external drive. The varying parameters are (a) the effective mass m_{eff} , (b) the fundamental frequency ω_m , and (c) the damping rate γ_m of the resonator. The values of the unaltered quantities in each figure are kept at constant value 1.

A widely used extension of the simple damped harmonic oscillator is the Duffing oscillator that introduces a nonlinear term proportional to x^3 into the EOM. Landau and Lifshitz [22] discuss the Duffing oscillator among other anharmonic oscillations. Micromechanical resonators can be manufactured from e.g. graphene or carbon nanotubes, and the study of their behaviour is an active field. Several types of micro- and nanomechanical resonators

that exhibit nonlinear behaviour are studied e.g. by Zaitsev et al. [23] and Eichler et al. [20]. I do not provide any derivation of these extended models here, but for example Zaitsev et al. [23] provide a clear and detailed derivation of the EOM of their nonlinearly dissipative doubly clamped beam oscillator.

2.2 Optomechanical system

In a full optomechanical system, the cavity element and mechanical motion are coupled which allows the study of interaction between matter and electromagnetic radiation, e.g. visible light. For example, mechanical motion can be introduced to a Fabry-Pérot setup by allowing one of the mirrors to be attached to a micro- or nanomechanical spring while the other is fixed in place, see Fig. 3a. The laser that is directed into the cavity exerts a radiation pressure force on the moving mirror thus causing it to vibrate. Because of the simple geometry of the Fabry-Pérot cavity, the average radiation pressure force caused by the momentum transfer of the cavity photons is easy to calculate. A single photon of the wavelength λ has a momentum of $p = 2\pi/\lambda$ with the unit convention $\hbar = 1$. Note that I use this convention throughout this work. Ideally the photon scatters back from the vibrating mirror thus transferring the momentum $|\Delta p| = 4\pi/\lambda$. The average radiation pressure force is determined by the momentum transfer of the average photon number $\langle a^\dagger a \rangle$ that happens during the time $\tau_c = 2L/c$ that it takes for a single photon to do a full round-trip in the cavity. Thus the radiation pressure force is

$$\langle F_{\text{rad}} \rangle = |\Delta p| \frac{\langle a^\dagger a \rangle}{\tau_c} = \frac{\omega_{\text{cav}}}{L} \langle a^\dagger a \rangle. \quad (2.7)$$

Here $a^{(\dagger)}$ is the annihilation (creation) operator of the single cavity mode.

An optical setup is not the only method of studying optomechanics. An equivalent electrical circuit, presented in Fig. 3b, can be constructed to study the microwave domain. A simple LC-circuit is known to behave like a harmonic oscillator, and therefore it can be used instead of the optical cavity to study a different frequency range. Mechanical motion is introduced to the system via a capacitor whose capacitance varies as a function of the displacement, and this capacitance as well as its impact on the LC-circuit can be measured. Note that the electric field between the capacitor plates and the magnetic field of the inductor consist of photons just like the visible light in the optical cavity, meaning that both kinds of setups can be used to study the same phenomena. Since the magnetic and electric fields appear in separate locations, the photons that they consist of are delocalized [24]. To model the effects of a heat bath environment, the harmonic oscillator circuit is coupled capacitively to a transmission line. The circuit analogs of the optomechanical system are not the focus of this thesis, however the quantization of electrical circuits is studied in detail in [24] and [25].

As mentioned above, to understand the physics in an optomechanical system, it is not enough to study the cavity and the mechanics as separate harmonic oscillators, each with their own fundamental mode. The optical cavity is coupled to the mechanical motion by attaching one of the mirrors to a spring that is forced to oscillate due to the radiation pressure force of the driving laser. Thus the separation, L , of the two mirrors of the cavity is affected which in turn, according to Eq. (2.1) changes the frequencies of the standing EM waves that are able to form inside the cavity resulting in different radiation pressure exerted on the mechanics. This feedback between the cavity and the mechanics

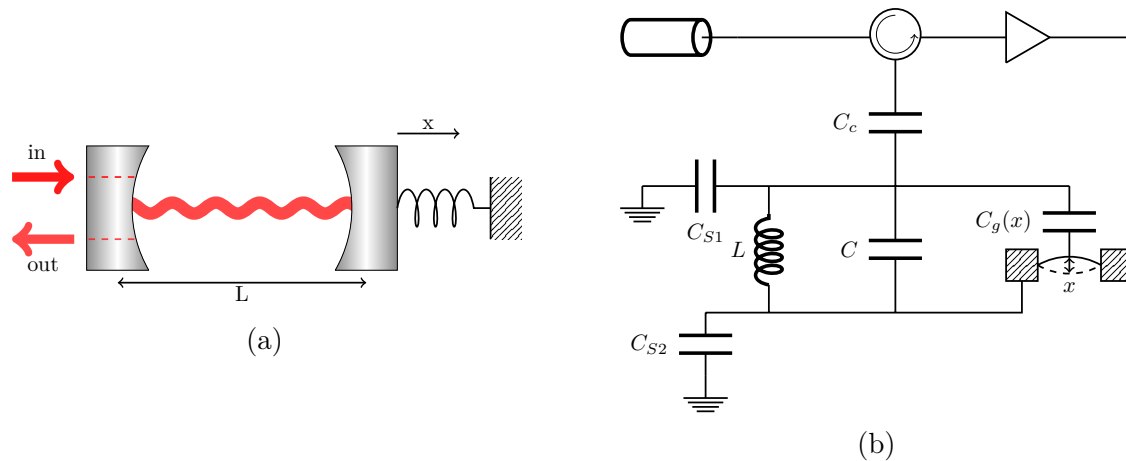


Figure 3: Schematical depictions of (a) an optical optomechanical system consisting of two highly reflective mirrors facing each other, the other being coupled to mechanical motion, and (b) an equivalent electrical circuit. The system-environment coupling is denoted by (a) “in” and “out” that represent the incoming laser and the escaping photons, respectively, (b) the transmission line to which the LC-circuit is capacitively coupled.

is known as *backaction* and it creates interesting nontrivial dynamics into the system. A way to solve the motion of an optomechanical setup coupled to a heat bath is introduced in Chap. 3 along with explicit exemplary calculations of the problem.

Let us consider one interesting application of optomechanical systems. The optomechanical coupling between the cavity and the mechanics can be used to cool down the mechanics [11], i.e. the phonon population of the mechanics can be decreased. Figure 4 illustrates three possible transitions that can occur between the number states of the optomechanical system. The cavity can be pumped using a laser with the frequency ω_p so that $\Delta = \omega_p - \omega_{\text{cav}} \approx -\omega_m$, where ω_{cav} is the dominating cavity frequency and ω_m is the frequency of the mechanics. This detuning Δ of the cavity is referred as the *red sideband* regime. In this sideband regime, the cavity can be excited to a higher energy level by allowing it to absorb the energy of a phonon. The cavity can then relax to a lower photon population. In the red sideband this process is the dominating one which leads to the cooling of the mechanics.

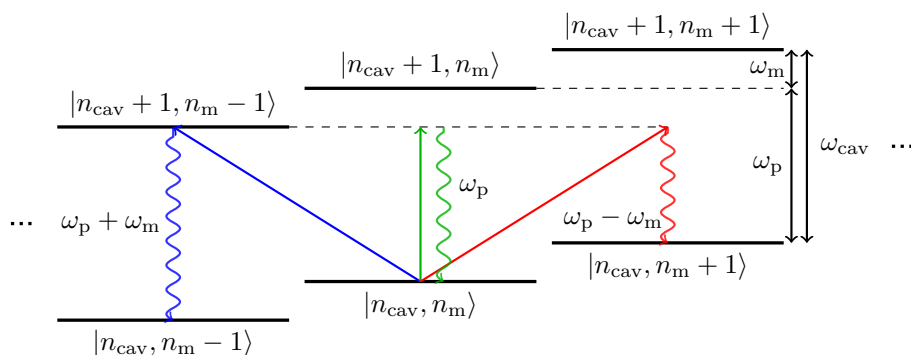


Figure 4: Schematical description of the possible transitions when the cavity is pumped at the frequency ω_p in terms of the phonon number n_m of the mechanics and the photon number n_{cav} of the cavity. Pumping at the red sideband makes the transition to the lower phonon number state (blue path in the figure) dominant thus cooling down the mechanics.

Open quantum systems

Optomechanical systems cannot be completely isolated from their environment. This has to be taken into account when measuring an observable of the open system to properly handle the effects of the environment on the system. In this Chapter, I focus on two ways of treating the time evolution of open quantum systems, the *Master equation* (ME) approach and the *input-output formalism*.

On one hand applying the input-output formalism on some open quantum system leads to a *quantum Langevin equation* (QLE) describing the time evolution of some operator of the system when the coupling between the system and its environment is known. On the other hand the ME approach gives the time evolution of the density operator of the system. These two seemingly different methods still describe the same phenomena and can be intuitively thought as the equivalents of a Heisenberg picture and a Schrödinger picture for open quantum systems.

The approach to open quantum systems in this work relies on the fact that the system is *Markovian*, meaning that the past states of the system do not influence its future. The concept of Markovianity is explored in Sec. 3.1, and the introduction to the subject mostly follows the discussion by Breuer et al. [26]. In Sec. 3.2, I discuss an introduction to the input-output formalism that is accompanied with calculations related to optomechanics presented in Sec. 3.3. The ME approach and its connection to the input-output formalism is discussed in Sec. 3.4.

3.1 The Markov process

Classically a Markovian process is defined so that the probability of the process to be in the state x_n at a time t_n is fully determined by the values x_{n-1} and t_{n-1} . In other words the states x_1, \dots, x_{n-2} at the times t_1, \dots, t_{n-2} play no role in determining the future of the system, a property which can be intuitively summarized by saying that the system has no memory.

The quantum mechanical description is a bit more subtle. By defining the trace norm of operator O as $\|O\| = \text{Tr}|O| = \text{Tr}\sqrt{O^\dagger O}$, the *trace distance* measuring the distance between two quantum states described by the density operators ρ_1 and ρ_2 is determined by [26]

$$D(\rho_1, \rho_2) = \frac{1}{2} \|\rho_1 - \rho_2\|. \quad (3.1)$$

The trace distance is a well-defined metric on the state space $\mathcal{S}(\mathcal{H})$ of the overall Hilbert

space \mathcal{H} since it satisfies the following criteria

$$D(\rho_1, \rho_2) \geq 0, \quad (3.2a)$$

$$D(\rho_1, \rho_2) = 0 \Leftrightarrow \rho_1 = \rho_2, \quad (3.2b)$$

$$D(\rho_1, \rho_2) = D(\rho_2, \rho_1), \quad (3.2c)$$

$$D(\rho_1, \rho_3) \leq D(\rho_1, \rho_2) + D(\rho_2, \rho_3), \quad (3.2d)$$

for all $\rho_1, \rho_2, \rho_3 \in \mathcal{S}(\mathcal{H})$. The first three conditions are satisfied trivially but the triangle inequality (3.2d) requires a short proof.

Since a density matrix is a Hermitian operator, the trace norm can also be defined as $\|\rho\| = \sum_i |\lambda_i|$, where $\lambda_i \in \mathbb{R}$ are the eigenvalues of ρ . Also the sum of two Hermitian operators is still Hermitian meaning that $\|\rho_1 - \rho_2\| = \sum_i |\lambda_{1,i} - \lambda_{2,i}|$. Now

$$\begin{aligned} D(\rho_1, \rho_2) + D(\rho_2, \rho_3) &= \frac{1}{2} \|\rho_1 - \rho_2\| + \frac{1}{2} \|\rho_2 - \rho_3\| \\ &= \frac{1}{2} \sum_i |\lambda_{1,i} - \lambda_{2,i}| + \frac{1}{2} \sum_i |\lambda_{2,i} - \lambda_{3,i}| \\ &\geq \frac{1}{2} \sum_i |\lambda_{1,i} - \lambda_{3,i}| \\ &= D(\rho_1, \rho_3), \end{aligned} \quad (3.3)$$

where the triangle inequality of \mathbb{R} is utilized.

Now that the trace distance is established as a metric in the state space, it can be used as a natural way of distinguishing two quantum states from each other, just like one would do for two points in \mathbb{R}^3 using the Euclidean metric. Suppose that a quantum system is prepared to either the state ρ_1 or ρ_2 with equal probabilities. Now the maximum probability of successfully determining the quantum state with a single quantum measurement is given by

$$P_{\max} = \frac{1}{2} [1 + D(\rho_1, \rho_2)]. \quad (3.4)$$

Note that the probability is well defined, since the trace distance is bounded from above, $D(\rho_1, \rho_2) \leq 1$, and the condition $D(\rho_1, \rho_2) = 1$ is satisfied only when ρ_1 and ρ_2 are orthogonal.

Let $\Phi : \mathcal{S}(\mathcal{H}) \rightarrow \mathcal{S}(\mathcal{H})$ be a completely positive and trace preserving map. The time evolution of an open quantum system from t_0 to $t > t_0$ can be expressed this way provided that initially the system and the environment are in an uncorrelated state. It can be shown that such a mapping is a contraction for the trace distance. This means that for all $\rho_1, \rho_2 \in \mathcal{S}(\mathcal{H})$ it holds that

$$D(\Phi\rho_1, \Phi\rho_2) \leq D(\rho_1, \rho_2). \quad (3.5)$$

This shows us that using any trace preserving and completely positive mapping does not help us to distinguish two quantum states from another.

Suppose now that two quantum states $\rho_1(0)$ and $\rho_2(0)$ are prepared and sent through a noisy channel Φ_t . The receiver gets the states $\Phi_t\rho_{1/2}(0) = \rho_{1/2}(t)$ obeying the relation (3.5), i.e.

$$D(\rho_1(t), \rho_2(t)) \leq D(\rho_1(0), \rho_2(0)). \quad (3.6)$$

One can see that the noisy channel makes the two quantum states less distinguishable, which can be interpreted as a loss of information from the studied open system to the environment over time. Analogously the increase in the trace distance over time can be interpreted as information flowing back to the system from the environment.

Now Markovianity can be properly defined. A quantum map $\Phi_t : \mathcal{S}(\mathcal{H}) \rightarrow \mathcal{S}(\mathcal{H})$, $\Phi_t \rho(0) = \rho(t)$, is Markovian if $D(\rho_1(t), \rho_2(t))$ decreases monotonically for all $\rho_{1/2}(0) \in \mathcal{S}(\mathcal{H})$ for all times $t \geq 0$.

Therefore a process is non-Markovian if there exist some initial states whose trace distance increases for some time interval $t_2 > t_1 \geq 0$, i.e. it is not enough to check the Markovianity condition for only two possible initial states to confirm the process to be Markovian. Instead, one has to consider every possible initial state to make sure that information cannot flow back to the system for some specific initial setup.

While Markovianity means the continuous loss of information from the system to the environment, in a non-Markovian process information can be transmitted to the environment and flow back at some later time. This means that some memory effects are present, since the state of the system is not only determined by its infinitesimally previous state but also some states earlier than that. Therefore, the Markovianity criterion can be expressed in a more intuitive manner. Markovian evolution is determined solely by the previous instant whereas in a non-Markovian process the system can be thought to have a memory of its past states that can then affect its time evolution at later times.

3.2 Input-output formalism

Consider now an isolated system, i.e. a system that does not interact with any other physical system. Thus the dynamics is entirely determined by the system itself. The Heisenberg equation of motion [15]

$$\frac{dO(t)}{dt} = i[H(t), O(t)] + \frac{\partial O(t)}{\partial t} \quad (3.7)$$

is enough to determine the complete time evolution of the operator O of an isolated system described by the Hamiltonian operator H . Both O and H are in the Heisenberg picture in this formulation, and the partial derivative denotes the time derivative with respect to the explicit time dependence. To briefly return to the optomechanical context, say that the cavity truly was isolated. Then the time evolution of the cavity field operator a would be described by trivial oscillation

$$\dot{a} = -i\omega_{\text{cav}}a \quad (3.8)$$

as given by Eqs. (2.3) and (3.7).

Naturally experimental setups are not ideal isolated systems that do not exchange any information with their environments. The loss mechanisms discussed above in Sec. 2.1 related to an optical cavity and mechanical oscillators are a clear manifestation of this. To take into account the effects of the environment, an approach that considers also the dynamics of the environment needs to be utilized. In other words the aim is to develop a quantum mechanical equation of motion for a system field operator that not only includes the isolated time evolution of the system but also the effects of the environment, see Fig. 5. As a prototypical example let us consider a harmonic oscillator coupled to a heat bath.

As we shall see in Secs. 3.3 and 4.1 the description developed here will provide important insight into optomechanical systems.

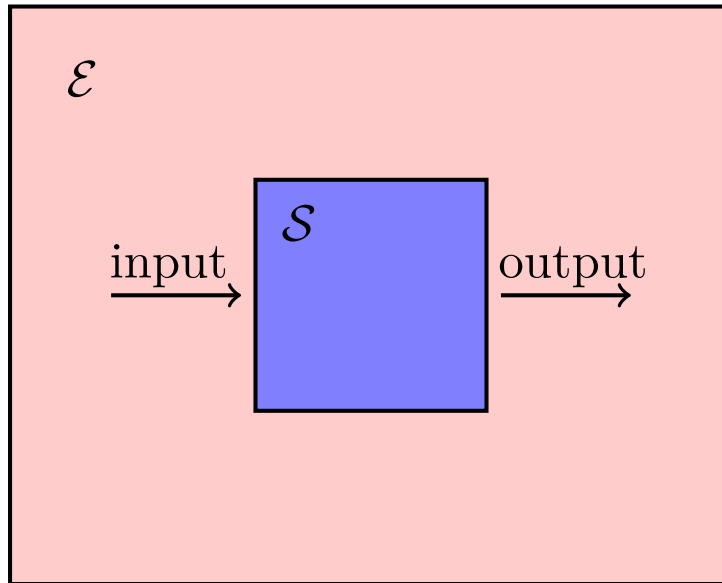


Figure 5: Schematic of the interaction between the system \mathcal{S} and the environment \mathcal{E} . An open quantum system can receive information from the surrounding heat bath (input) as well as lose some back to the environment (output).

The approach suited for treating the time evolution of damped open quantum systems where explicit inputs from the environment are considered was developed by Gardiner and Collett [27], and their method of constructing a stochastic quantum Langevin equation has since become a widely used practice in the study of open quantum systems [28, 29]. Note that here I lay out the general framework of the method and provide some simple results. An explicit calculation using this method for a slightly different system-environment coupling is provided in Appendix A.

Let the environment be modeled by a set of noninteracting bosonic harmonic oscillators described by the Hamiltonian

$$H_E = \sum_n \omega_n c_n^\dagger c_n, \quad (3.9)$$

where the annihilation (creation) operator of the n th mode is denoted by c_n (c_n^\dagger).

Let the coupling between the environment and the system be described by the following Hamiltonian

$$H_I = i \sum_n g_n [c_n^\dagger a - c_n a^\dagger]. \quad (3.10)$$

The strength of the coupling between the system field operator and the n th mode of the environment is given by g_n .

Neither the system nor the environment are isolated systems, meaning that Heisenberg EOMs, given by Eq. (3.7), cannot be formally constructed for them. However, this can be done for both the environment and the system field operators when the whole “universe”, i.e. the system, the environment, and their mutual interaction, is considered as an isolated system whose Hamiltonian is

$$H = H_S + H_E + H_I, \quad (3.11)$$

where H_S is the Hamiltonian of the open quantum system that is not required to be specified for this formalism. The EOMs of the environment and the system degrees of freedom are given by

$$\dot{c}_n(t) = i[H, c_n] = -i\omega_n c_n + g_n a, \quad (3.12)$$

$$\dot{a}(t) = i[H, a] = i[H_S, a] - \sum_n g_n c_n, \quad (3.13)$$

which represent the coherent transfer of excitations between the system and the environment.

The dynamics of the bath degrees of freedom can be expressed in terms of an initial condition at $t_0 < t$ and the state of the system at times $t' < t$

$$c_n(t) = e^{-i\omega_n(t-t_0)} c_n(t_0) + g_n \int_{t_0}^t e^{-i\omega_n(t-t')} a(t') dt'. \quad (3.14)$$

Analogously one could have expressed $c_n(t)$ using the state of the system at times $t' > t$

$$c_n(t) = e^{-i\omega_n(t-t_1)} c_n(t_1) - g_n \int_t^{t_1} e^{-i\omega_n(t-t')} a(t') dt', \quad (3.15)$$

where some final condition is determined at $t_1 > t$.

Let us plug the solution of the environment degree of freedom (3.14) back into the EOM for the system operator (3.13) to get

$$\dot{a}(t) = i[H_S, a] - \sum_n g_n e^{-i\omega_n(t-t_0)} c_n(t_0) - \sum_n g_n^2 \int_{t_0}^t e^{-i\omega_n(t-t')} a(t') dt'. \quad (3.16)$$

Following Gardiner and Collett [27], I impose that the coupling strength between the system and a particular mode of the environment does not depend on the frequency of said mode. This assumption, called the *first Markov approximation* [27], allows us to define the coupling constant κ so that

$$(g_n)^2 = \frac{\kappa}{2\pi D}, \quad (3.17)$$

where D is the density of states of the modes, which I assume to be frequency independent, i.e. $n = \omega_n D = \omega_n \partial n / \partial \omega_n$.

This gives us a general quantum Langevin equation for any open quantum system that is linearly coupled to its environment

$$\dot{a}(t) = i[H_S, a(t)] - \frac{\kappa}{2} a(t) + \sqrt{\kappa} a_{\text{in}}(t), \quad (3.18)$$

where the *input field* is defined as

$$a_{\text{in}} = -\sqrt{\frac{1}{2\pi D}} \sum_n e^{-i\omega_n(t-t_0)} c_n(t_0). \quad (3.19)$$

The input and output approaches are related to each other by a simple time-reversal symmetry which gives the output of the system to the environment in the form

$$a_{\text{out}} = a_{\text{in}} - \sqrt{\kappa} a \quad (3.20)$$

due to the sign difference between the integrals of Eqs. (3.14) and (3.15).

As it is possible to see from (3.18), the assumption of frequency independent system-environment coupling guarantees that the dynamics of the system is Markovian in the sense that the dynamics is entirely local in time. The evolution of the system at time t does not depend on its previous states at times $t' < t$, since all operators in the QLE are defined at the same instant.

The term $(-\kappa/2)a$ is the damping of the system, since one can see that it results in a term proportional to $e^{-\frac{\kappa}{2}t}$ in the solution of a . Thus such a term decreases the amplitude of a over time, effectively dissipating energy from the system to the environment. Notice that the external damping of the system arises from the system-environment interaction naturally without any prior knowledge of the system itself.

If the system is just a cavity described by the Hamiltonian of the harmonic oscillator (2.3), the QLE of this system is

$$\dot{a}(t) = -i\omega_{\text{cav}}a(t) - \frac{\kappa}{2}a(t) + \sqrt{\kappa}a_{\text{in}}(t), \quad (3.21)$$

where Eq. (3.8) is used to get the time evolution of an isolated cavity with dominating frequency ω_{cav} . This QLE is not limited to optical cavities, since any harmonic oscillator such as a simple mechanical resonator also obeys the above equation provided that it is coupled with its environment similarly.

The QLE (3.21) can easily be solved using the Fourier transform $a(\omega) = \int dt e^{i\omega t} a(t)$ that gives us

$$a(\omega) = \frac{\sqrt{\kappa}}{i(\omega_{\text{cav}} - \omega) + \frac{\kappa}{2}} a_{\text{in}}(\omega) \quad (3.22)$$

showing the response of the cavity to an external field. In terms of the output of the cavity, the response can be written as

$$a(\omega) = \frac{\sqrt{\kappa}}{i(\omega_{\text{cav}} - \omega) - \frac{\kappa}{2}} a_{\text{out}}(\omega). \quad (3.23)$$

3.3 Linear formulation of optomechanics

In the discussion above in Sec. 3.2, I focus only on the time evolution of a cavity. Let us now discuss the full optomechanical system. Consider an optical cavity (operator a) coupled to mechanics (operator b) by allowing one of the cavity mirrors to oscillate. Assume that both the cavity and the mechanics have only one dominant mode. Let us consider the coupling up to linear order

$$\omega_{\text{cav}}(x) \approx \omega_{\text{cav}}(x_0) + \left. \frac{\partial \omega_{\text{cav}}}{\partial x} \right|_{x_0} (x - x_0). \quad (3.24)$$

In this case the Hamiltonian can be written as [11]

$$H_{\text{opt}} = \omega_{\text{cav}} a^\dagger a + \omega_{\text{m}} b^\dagger b - g_0 a^\dagger a (b^\dagger + b), \quad (3.25)$$

where g_0 is the single photon coupling strength. Note that the zero-point energies, presented in Eq. (2.3), of the cavity and the mechanics are omitted. The form of the coupling

term makes intuitive sense based on the above discussion about radiation pressure. $a^\dagger a$ is the photon number of the cavity and it is related to the average radiation pressure on the mechanics by Eq. (2.7). $b^\dagger + b$ that is proportional to the displacement of the mechanical oscillator, is coupled with the radiation pressure force.

Equation (3.18) can be utilized to write the QLEs of the field operators of the cavity and the mechanics provided that both are linearly coupled to the environment

$$\dot{a} = -i\omega_{\text{cav}}a - \frac{\kappa}{2}a + ig_0a(b^\dagger + b) + \sqrt{\kappa}a_{\text{in}}, \quad (3.26a)$$

$$\dot{b} = -i\omega_{\text{m}}b - \frac{\gamma}{2}b + ig_0a^\dagger a + \sqrt{\gamma}b_{\text{in}}, \quad (3.26b)$$

where κ and γ determine the strengths of the cavity-environment and mechanics-environment couplings, respectively.

Assuming that the coherent laser pump driving the optical cavity is strong, the cavity field operator (input field) can be linearly decomposed as

$$a_{(\text{in})} = \alpha_{(\text{in})} + \delta a_{(\text{in})}, \quad (3.27)$$

where α is the average coherent amplitude of a rotating at the frequency of the pump ω_{p} , and δa is a fluctuating term.

A similar decomposition can also be written for the mechanics (and its input field)

$$b_{(\text{in})} = \beta_{(\text{in})} + \delta b_{(\text{in})}. \quad (3.28)$$

Here I assume that the mechanical system is not driven on average, i.e. $\beta_{\text{in}} = 0$.

The zeroth order approximations in terms of the fluctuations of the EOM (3.26) can be written, and they give the following steady state solutions

$$\alpha = \frac{\sqrt{\kappa}\alpha_{\text{in}}}{\frac{\kappa}{2} - i[\Delta + g_0(\beta^* + \beta)]}, \quad (3.29a)$$

$$\beta = \frac{ig_0|\alpha|^2}{\frac{\gamma}{2} + i\omega_{\text{m}}}, \quad (3.29b)$$

where $\Delta = \omega_{\text{p}} - \omega_{\text{cav}}$ is the detuning of the cavity. Since α and β represent the average field quantities for the cavity and the mechanical modes, $|\alpha|^2$ and $|\beta|^2$ can be identified as the average number of photons in the cavity and phonons in the mechanics.

The detuning Δ determines two important regimes known as the *red* and *blue detuned sidebands*, respectively. By adjusting the detuning, its size can be fixed to match the fundamental mechanical mode ω_{m} . This way the system consists of two harmonic oscillators with the same fundamental frequencies enabling them to exchange quanta. The red detuned regime, on one hand, is characterized by the condition $\Delta \approx -\omega_{\text{m}}$ while the blue, on the other hand, corresponds to $\Delta \approx \omega_{\text{m}}$, see Fig. 6. In the blue sideband the mechanical resonator absorbs energy causing the amplification of the resonance, and conversely in the red sideband energy is emitted into the cavity resulting in effective cooling of the mechanics [11]. The quantum theory of cooling is not explored further here, however Marquardt et al. [30] provide a review of the subject. As a short sidenote, it is important to distinguish the two sidebands when performing the rotating wave approximation (RWA)

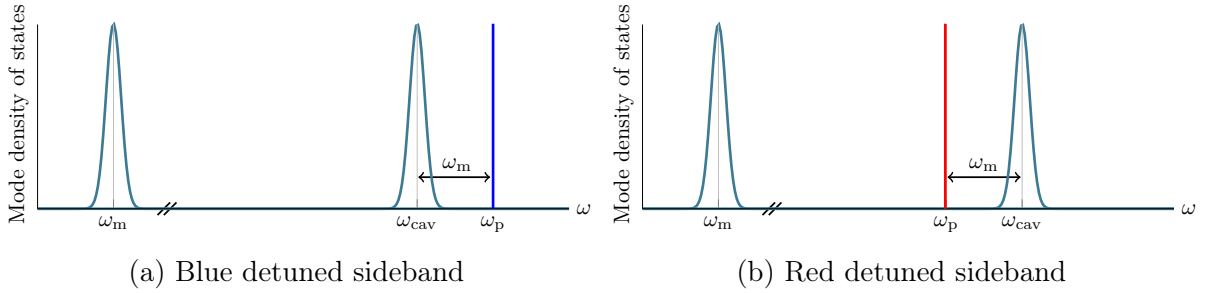


Figure 6: Schematical description of optomechanical detuning sidebands in terms of mode densities of states of the mechanics, the cavity, and the laser pump. (a) In the blue detuned sideband the mechanical motion is amplified whereas in (b) the red detuned sideband the mechanics are cooled down.

on the Hamiltonian (3.25) since this approximation in different regimes results in different dominating terms of the optomechanical coupling.

The first order approximation of Eq. (3.26) with respect to the fluctuations can be constructed. This approximation is expanded around the steady state solution meaning that the zeroth order terms in fluctuations vanish. Thus I get

$$\delta\dot{a} = \left[-i\omega_{\text{cav}} - \frac{\kappa}{2} + ig_0(\beta^* + \beta) \right] \delta a + ig_0\alpha(\delta b^\dagger + \delta b) + \sqrt{\kappa}\delta a_{\text{in}}, \quad (3.30a)$$

$$\delta\dot{b} = \left(-i\omega_m - \frac{\gamma}{2} \right) \delta b + ig_0(\alpha^*\delta a + \alpha\delta a^\dagger) + \sqrt{\gamma}\delta b_{\text{in}}, \quad (3.30b)$$

and similar Eqs. for δa^\dagger and δb^\dagger . These EOMs show explicitly the optomechanical back-action since the time evolution of the cavity field operator depends on the mechanics and vice versa.

The QLEs (3.30a) and (3.30b) can be solved by Fourier transforming the equations which turns the differential equations into algebraic ones. Short proof of this is provided in Appendix D as well as the complete definitions of the Fourier transforms used in this work. This way the optomechanical response function can be calculated to gain insight on how the system responds to an external force, similar to the case of the mechanical resonator presented above in Sec. 2.1. More on linear response theory can be found in standard textbooks such as [31].

In the red sideband, the interaction term simplifies to $-g_0(a^\dagger b + ab^\dagger)$, whereas in the blue sideband the interaction between the cavity and the mechanics can be approximated as $-g_0(a^\dagger b^\dagger + ab)$. These are the resonant terms in their respective sidebands, while the nonresonant ones are discarded due to the RWA. In the red sideband, the cavity and the mechanics are able to exchange quanta allowing the mechanics to cool down [11]. On the contrary, the interaction term corresponding to the blue sideband is related to parametric amplification of the mechanics [13].

For completeness, let us calculate the optomechanical response in both red and blue sideband regimes. In the red sideband regime, the first order approximation with respect to the fluctuations is

$$\delta\dot{a} = \left[-i\omega_{\text{cav}} - \frac{\kappa}{2} + ig_0\beta^* \right] \delta a + ig_0\alpha\delta b + \sqrt{\kappa}\delta a_{\text{in}}, \quad (3.31a)$$

$$\delta\dot{b} = \left[-i\omega_m - \frac{\gamma}{2} \right] \delta b + ig_0\alpha^*\delta a + \sqrt{\gamma}\delta b_{\text{in}}. \quad (3.31b)$$

Comparing these red sideband resolved QLEs to the full EOMs (3.30) one can see that δa and δb^\dagger are no longer coupled with each other, and neither are δa^\dagger and δb . Fourier transforming these EOMs gives

$$\begin{pmatrix} \chi_{\text{cav}}^{-1} & -iG \\ -iG^* & \chi_{\text{m}}^{-1} \end{pmatrix} \begin{pmatrix} \delta a_\omega \\ \delta b_\omega \end{pmatrix} = \begin{pmatrix} \sqrt{\kappa} \delta a_{\text{in},\omega} \\ \sqrt{\gamma} \delta b_{\text{in},\omega} \end{pmatrix}, \quad (3.32)$$

where

$$G = g_0 \alpha, \quad (3.33a)$$

$$\chi_{\text{cav}}^{-1} = -i(\omega - \omega_{\text{cav}}) + \frac{\kappa}{2} - ig_0 \beta^*, \quad (3.33b)$$

$$\chi_{\text{m}}^{-1} = -i(\omega - \omega_{\text{m}}) + \frac{\gamma}{2}. \quad (3.33c)$$

Recall that $|\alpha|^2$ is the average photon number of the cavity. Now the optomechanical coupling strength G can be expressed in terms of the field amplitude provided that $\alpha \in \mathbb{R}$. Experimental setups have been developed in attempts to increase the optomechanical coupling strength in order to achieve nonlinear quantum effects that start to become observable in the strongly coupled regime of $g_0 > \kappa$ [11, 32].

The effect of a drive on the cavity and the mechanics can be formulated in the red sideband regime

$$\begin{pmatrix} \delta a_\omega \\ \delta b_\omega \end{pmatrix} = \frac{1}{\chi_{\text{cav}}^{-1} \chi_{\text{m}}^{-1} + |G|^2} \begin{pmatrix} \chi_{\text{m}}^{-1} & iG \\ iG^* & \chi_{\text{cav}}^{-1} \end{pmatrix} \begin{pmatrix} \sqrt{\kappa} \delta a_{\text{in},\omega} \\ \sqrt{\gamma} \delta b_{\text{in},\omega} \end{pmatrix}. \quad (3.34)$$

This shows us that the decoupling that is achieved by going to the sideband resolved regime simplifies the response of the optomechanical system significantly. Here δa is only coupled with δb and vice versa.

A similar calculation can be performed in the blue sideband regime. The EOMs of the optomechanical system up to first order in fluctuating terms are

$$\delta \dot{a} = \left[-i\omega_{\text{cav}} - \frac{\kappa}{2} + ig_0 \beta \right] \delta a + ig_0 \alpha \delta b^\dagger + \sqrt{\kappa} \delta a_{\text{in}}, \quad (3.35a)$$

$$\delta \dot{b} = \left[-i\omega_{\text{m}} - \frac{\gamma}{2} \right] \delta b + ig_0 \alpha \delta a^\dagger + \sqrt{\gamma} \delta b_{\text{in}}. \quad (3.35b)$$

Fourier transform the EOMs of δa and δb^\dagger to get

$$\begin{pmatrix} \tilde{\chi}_{\text{cav}}^{-1} & -iG \\ iG^* & \tilde{\chi}_{\text{m}}^{-1} \end{pmatrix} \begin{pmatrix} \delta a_\omega \\ \delta b_{-\omega}^\dagger \end{pmatrix} = \begin{pmatrix} \sqrt{\kappa} \delta a_{\text{in},\omega} \\ \sqrt{\gamma} \delta b_{\text{in},-\omega}^\dagger \end{pmatrix}, \quad (3.36)$$

where

$$\tilde{\chi}_{\text{cav}}^{-1} = -i(\omega - \omega_{\text{cav}}) + \frac{\kappa}{2} - ig_0 \beta, \quad (3.37a)$$

$$\tilde{\chi}_{\text{m}}^{-1} = -i(\omega + \omega_{\text{m}}) + \frac{\gamma}{2}. \quad (3.37b)$$

Note that the frequency dependence of the Hermitian conjugate of δb is $-\omega$ to keep the Fourier transforms consistent.

The response of the optomechanical system is thus in the blue sideband regime

$$\begin{pmatrix} \delta a_\omega \\ \delta b_{-\omega}^\dagger \end{pmatrix} = \frac{1}{\tilde{\chi}_{\text{cav}}^{-1} \tilde{\chi}_{\text{m}}^{-1} - |G|^2} \begin{pmatrix} \tilde{\chi}_{\text{m}}^{-1} & iG \\ -iG^* & \tilde{\chi}_{\text{cav}}^{-1} \end{pmatrix} \begin{pmatrix} \sqrt{\kappa} \delta a_{\text{in},\omega} \\ \sqrt{\gamma} \delta b_{\text{in},-\omega}^\dagger \end{pmatrix}. \quad (3.38)$$

3.4 Master equation approach

Quantum Langevin equations are one way of studying the time evolution of open quantum systems. An alternative method is the Master equation approach that describes the time evolution of the density operator of the studied system. Here I show how these two descriptions can be linked, and in the following I derive the ME for a system whose QLE is already known to be (3.18). The derivation of the Master equation presented here is based on the quantum information lecture notes by Preskill [33].

Let us first focus on an isolated quantum system. The time evolution of a pure quantum state $|\Psi(t)\rangle$ of the system is governed by the Schrödinger equation [34]

$$i\frac{\partial}{\partial t}|\Psi(t)\rangle = H|\Psi(t)\rangle, \quad (3.39)$$

where H is the Hamiltonian of the system. Since in the Schrödinger picture the states evolve in time whereas the operators do not, we can consider the operator $U(t, t_0)$ that generates the time evolution for the state $|\Psi\rangle$ as

$$|\Psi(t)\rangle = U(t, t_0)|\Psi(t_0)\rangle. \quad (3.40)$$

We can thus write the Schrödinger equation as

$$i\frac{\partial}{\partial t}U(t, t_0) = HU(t, t_0) \quad (3.41)$$

giving the explicit form of the time-evolution operator

$$U(t, t_0) = e^{-iH(t-t_0)}. \quad (3.42)$$

The time evolution of the state $|\Psi(t)\rangle$ over an infinitesimal time interval dt can therefore be expressed up to linear order by expanding the operator exponential in powers of $-iH$

$$|\Psi(t+dt)\rangle = (\mathbb{1} - iHdt)|\Psi(t)\rangle. \quad (3.43)$$

If we now consider a general state, the general form of its density operator ρ is [35]

$$\rho(t) = \sum_n p_n |\Psi_n(t)\rangle \langle \Psi_n(t)|, \quad (3.44)$$

where the coefficients p_n satisfy $p_n \geq 0$ for all n and $\sum_n p_n = 1$.

Considering Eq. (3.43), one gets

$$\dot{\rho}(t) = -i[H, \rho(t)]. \quad (3.45)$$

This EOM can be seen as an alternative formulation of the Schrödinger equation, both of them expressing the idea that the dynamics of an isolated system is generated by the system Hamiltonian.

Consider an open quantum system with a density operator $\rho_S(t) \in \mathcal{S}(\mathcal{H})$ where $\mathcal{S}(\mathcal{H})$ is the state space of the Hilbert space \mathcal{H} . Input-output formalism utilizes the assumption that the time evolution is Markovian, see (3.17), and also the following derivation of the Master equation is formulated in terms of Markovian evolution. Above in Sec. 3.1, the definition of Markovianity implies that the time evolution of a state of a system during

the next infinitesimal interval is determined by the current state of the system, i.e. there are no memory effects. Let $\varepsilon : \mathcal{S}(\mathcal{H}) \rightarrow \mathcal{S}(\mathcal{H})$ be a Markovian quantum channel, meaning that over an infinitesimal time interval it operates on the density operator of the system in the following way

$$\rho_S(t + dt) = \varepsilon_{dt}[\rho_S(t)]. \quad (3.46)$$

Because of the imposed Markovianity, ε_{dt} makes the quantum states on which it operates less distinguishable, cf. Eq. (3.6). Therefore the quantum channel ε_{dt} has to be a contraction for all instants for it to be Markovian, i.e. ε_{dt} is required to be completely positive and trace preserving.

Up to linear order in time the quantum channel ε_{dt} has the form

$$\varepsilon_{dt} = \mathbb{1} + \mathcal{L}dt \quad (3.47)$$

where \mathcal{L} is a linear mapping $\mathcal{L} : \mathcal{S}(\mathcal{H}) \rightarrow \mathcal{S}(\mathcal{H})$ called the *Lindblad superoperator*. This linearization of the quantum channel implies that

$$\dot{\rho}_S(t) = \mathcal{L}[\rho_S(t)]. \quad (3.48)$$

Suppose that the system evolves during the interval $[0, t]$ and let us divide this interval into n subintervals of equal length. If the length of an individual subinterval approaches zero, the definition (3.46) of Markovian evolution can be applied over each infinitesimal subinterval in succession. Using the linearized form (3.47) of ε_{dt} gives

$$\rho_S(t) = \lim_{n \rightarrow \infty} \left(\mathbb{1} + \frac{\mathcal{L}t}{n} \right)^n [\rho_S(0)] = e^{\mathcal{L}t} [\rho_S(0)] \quad (3.49)$$

assuming that the Lindblad superoperator does not depend on time.

Therefore the determination of the dynamics of the open quantum system discussed here corresponds to the determination of the Lindblad superoperator \mathcal{L} . In order to achieve this, I start by describing the dynamics of the system (S) and the environment (E) in terms of the unitary dynamics of a globally isolated quantum system.

Assume that the system and the environment are not initially entangled, i.e. the state of the system and the environment together can be expressed as a product state

$$|\Psi\rangle_S \otimes |0\rangle_E. \quad (3.50)$$

The unitary time evolution operator, denoted U , may entangle the system with the environment over time. Let $\{|\mu\rangle_E\}$ be an orthonormal basis of the environment. Expanding in the basis of the environment, U operates so that

$$U : |\Psi\rangle_S \otimes |0\rangle_E \mapsto \sum_{\mu} M_{\mu} |\Psi\rangle_S \otimes |\mu\rangle_E, \quad (3.51)$$

where the operators $\{M_{\mu}\}$ are called *Kraus operators*.

Since U is unitary, the completeness relation for the Kraus operators can be derived

$$\begin{aligned} 1 &= \left| |\Psi\rangle_S \otimes |0\rangle_E \right|^2 = \left| \sum_{\mu} M_{\mu} |\Psi\rangle_S \otimes |\mu\rangle_E \right|^2 \\ &= \sum_{\mu, \gamma} \langle \Psi | M_{\mu}^{\dagger} M_{\gamma} | \Psi \rangle_S \langle \mu | \gamma \rangle_E = \sum_{\mu} \langle \Psi | M_{\mu}^{\dagger} M_{\mu} | \Psi \rangle_S, \quad \forall |\Psi\rangle_S. \end{aligned} \quad (3.52)$$

This implies that

$$\mathbb{1} = \sum_{\mu} M_{\mu}^{\dagger} M_{\mu}. \quad (3.53)$$

Initially the total (S+E) density operator is given by

$$\rho_{\text{SE}}(0) = \rho_{\text{S}}(0) \otimes \rho_{\text{E}}(0) = (|\Psi\rangle_{\text{S}} \otimes |0\rangle_{\text{E}}) ({}_{\text{S}}\langle\Psi| \otimes {}_{\text{E}}\langle 0|). \quad (3.54)$$

The unitary mapping entangling the system and the environment is known (3.51), and now the general density operator of the combined system and the environment is

$$\rho_{\text{SE}} = \sum_{\mu\gamma} (M_{\mu} |\Psi\rangle_{\text{S}} \otimes |\mu\rangle_{\text{E}}) ({}_{\text{S}}\langle\Psi| M_{\gamma}^{\dagger} \otimes {}_{\text{E}}\langle\gamma|). \quad (3.55)$$

Tracing out the degrees of freedom of the environment gives us the *operator-sum representation* of the quantum channel that describes the evolution of the system density operator. The evolution during an infinitesimal time interval is

$$\rho_{\text{S}}(t + dt) = \varepsilon_{dt} [\rho_{\text{S}}(t)] = \sum_{\mu} M_{\mu} \rho_{\text{S}}(t) M_{\mu}^{\dagger}. \quad (3.56)$$

If the system does not undergo any quantum jumps during the infinitesimal interval dt , the Kraus operator corresponding to that is

$$M_0 = \mathbb{1} + (-iH_{\text{S}} + K) dt, \quad (3.57)$$

where the system Hamiltonian H_{S} and the operator K are Hermitian. On the other hand, if the system undergoes quantum jumps, these are represented by M_{μ} , $\mu \in \mathbb{N}$, so that

$$M_{\mu} = L_{\mu} dB, \quad \mu \in \mathbb{N}. \quad (3.58)$$

Here L_{μ} is a *Lindblad operator* or a *quantum jump operator* and dB is a Wiener process. More on stochastic calculus is presented, e.g. by Gardiner and Collett [27].

We can show that these definitions are consistent with the evolution of an isolated system in the limit where no quantum jumps occur. The completeness relation of the Kraus operators (3.53) can be used to get

$$\mathbb{1} = \sum_{\mu} M_{\mu}^{\dagger} M_{\mu} = \mathbb{1} + \left(2K + \sum_{\mu \in \mathbb{N}} L_{\mu}^{\dagger} L_{\mu} \right) dt + \mathcal{O}(dt^2), \quad (3.59)$$

which implies that

$$K = -\frac{1}{2} \sum_{\mu \in \mathbb{N}} L_{\mu}^{\dagger} L_{\mu}. \quad (3.60)$$

Now we see that when the system is isolated and no jumps occur, i.e. $M_{\mu} = 0$, $\mu \in \mathbb{N}$, the isolated time evolution presented in Eq. (3.45) is recovered from the operator-sum representation (3.56).

By plugging in Eqs. (3.57), (3.58) and (3.60) to the operator-sum representation (3.56), a short calculation yields

$$\begin{aligned} \rho_{\text{S}}(t + dt) = & \rho_{\text{S}}(t) - i[H_{\text{S}}, \rho_{\text{S}}(t)] dt \\ & + \left[\sum_{\mu \in \mathbb{N}} L_{\mu} \rho_{\text{S}}(t) L_{\mu}^{\dagger} - \frac{1}{2} \{ \rho_{\text{S}}(t), L_{\mu}^{\dagger} L_{\mu} \} \right] dt + \mathcal{O}(dt^2). \end{aligned} \quad (3.61)$$

Therefore the Master equation can be written in the form

$$\dot{\rho}_S = \mathcal{L}[\rho_S] = -i[H_S, \rho_S] + \sum_{\mu \in \mathbb{N}} L_\mu \rho_S L_\mu^\dagger - \frac{1}{2} \{\rho_S, L_\mu^\dagger L_\mu\}. \quad (3.62)$$

To explicitly express the ME for a specific system, one still needs to know the form of the Lindblad operators. The method outlined above allows me to form the QLE for the system. Since it is possible to construct the operator-sum representation of a quantum channel acting on the field operator of the system in the Heisenberg picture using the same Kraus operators as for the density operator, I can pick the Kraus operators so that the QLE is satisfied. The Master equation is then obtained by plugging in the same Kraus operators in the operator-sum representation of the quantum channel acting on the density operator in the Schrödinger picture (3.56).

We can use the fact that Heisenberg and Schrödinger pictures need to provide the same expectation value for observables to determine the link between the QLE and the ME. Let φ_{dt} be a superoperator determining the infinitesimal time evolution of a system field operator A in the Heisenberg picture. Now using the cyclic property of trace

$$\begin{aligned} \langle A \rangle_{\text{Hei}} &= \text{Tr}(\varphi_{dt}[A]\rho) = \text{Tr}\left(\sum_{\mu} M_{\mu}^{\dagger} A M_{\mu} \rho\right) \\ &= \text{Tr}\left(A \sum_{\mu} M_{\mu} \rho M_{\mu}^{\dagger}\right) = \text{Tr}(A \varepsilon_{dt}[\rho]) = \langle A \rangle_{\text{Sch}}. \end{aligned} \quad (3.63)$$

φ_{dt} is therefore the adjoint of ε_{dt} and I denote it by $\varepsilon_{dt}^{\dagger}$. This implies that, in the Heisenberg picture, the infinitesimal time evolution of an operator of an open quantum system can be expressed as

$$A(t+dt) = \varepsilon_{dt}^{\dagger}[A(t)] = \sum_{\mu} M_{\mu}^{\dagger} A(t) M_{\mu}. \quad (3.64)$$

Let us determine the Master equation of a linearly dissipative system described by the QLE (3.18). Slight modifications to the expressions Kraus operators given by (3.57) and (3.58) are needed to correctly express the input field terms of the QLE. Let us take the zeroth Kraus operator to be

$$M_0 = \mathbb{1} + LdB + (-iH_S + K)dt, \quad (3.65)$$

where L has dimensions of \sqrt{dt} and dB is a Wiener process. Assume that the other Kraus operators are higher order in dt . Taking the terms up to $\mathcal{O}(dt)$ in time, the completeness relation of the Kraus operators (3.53) implies that

$$L = -L^{\dagger}, \quad (3.66a)$$

$$K = -\frac{1}{2}L^{\dagger}L + \mathcal{O}(dt^{\frac{3}{2}}). \quad (3.66b)$$

The expression of M_0 given in Eq. (3.65) can be inserted back into the operator-sum representation (3.64) leading to the following expression for the operator a

$$\begin{aligned} a(dt) &= \varepsilon_{dt}^{\dagger}[a(0)] = \varepsilon_{dt}^{\dagger}[a_0] \\ &= a_0 + i[H_S, a_0]dt + a_0 LdB + L^{\dagger}a_0 dB \\ &\quad + L^{\dagger}a_0 LdB^2 - \frac{1}{2}\{a_0, L^{\dagger}L\}dB^2 + \mathcal{O}(dt^{\frac{3}{2}}) \\ &= a_0 + i[H_S, a_0]dt + [a_0, L]dB - La_0 LdB^2 + \frac{1}{2}\{a_0, L^2\}dB^2 + \mathcal{O}(dt^{\frac{3}{2}}). \end{aligned} \quad (3.67)$$

The constraints of L are now that L needs to be anti-Hermitian and the above expression has to coincide with the QLE (3.18). Since L describes the quantum jumps of the system induced by the environment, input field terms should be included as a part of it. One can consider the term $a_{\text{in}}^\dagger a_{\text{in}} dB^2$ as a flux of particles from the environment to the system. With the ansatz

$$L = \sqrt{\kappa} \left(a_0^\dagger a_{\text{in}} - a_0 a_{\text{in}}^\dagger \right) dB, \quad (3.68)$$

the following commutator gives the input term of the linear QLE

$$[a_0, L] dB = \sqrt{\kappa} a_{\text{in}} dt, \quad (3.69)$$

where standard bosonic commutation relations [15] are used as well as the fact that a commutes with a_{in} because the input field does not contain any system field operators. Using these commutation relations repeatedly reveals that

$$\left[-La_0L + \frac{1}{2} \{a_0, L^2\} \right] dt = -\frac{\kappa}{2} a_0 [a_{\text{in}}, a_{\text{in}}^\dagger] dt^2 \quad (3.70)$$

Since the input field obeys the commutation relation

$$[a_{\text{in}}(t), a_{\text{in}}^\dagger(t')] = \delta(t - t') \quad (3.71)$$

provided that the processes are considered to be Markovian [19], I can write

$$[a_{\text{in}} dt, a_{\text{in}}^\dagger dt] = dt. \quad (3.72)$$

Collecting the terms from Eqs. (3.69) and (3.70) shows that

$$a(dt) = i[H_S, a_0] dt - \frac{\kappa}{2} a_0 dt + \sqrt{\kappa} a_{\text{in}} dt, \quad (3.73)$$

i.e. the choice of the form of the zeroth Kraus operator (3.65) and the Lindblad operator (3.68) gives the form of the QLE explicitly derived from Eq. (3.18) up to the first order. If I use the same Kraus operator to get the time evolution of the density operator, I obtain

$$\begin{aligned} \rho_S(t + dt) = & \rho_S - i[H_S, \rho_S] dt \\ & - \sqrt{\kappa} [\rho_S, a^\dagger] \langle a_{\text{in}} \rangle dt + \sqrt{\kappa} [\rho_S, a] \langle a_{\text{in}}^\dagger \rangle dt \\ & + \kappa \left[\langle a_{\text{in}} a_{\text{in}} \rangle \left(-a^\dagger \rho_S a^\dagger + \frac{1}{2} \{ \rho_S, a^{\dagger 2} \} \right) dt \right] dt \\ & + \kappa \left[\langle a_{\text{in}}^\dagger a_{\text{in}}^\dagger \rangle \left(-a \rho_S a + \frac{1}{2} \{ \rho_S, a^2 \} \right) dt \right] dt \\ & + \kappa \left[\langle a_{\text{in}}^\dagger a_{\text{in}} \rangle \left(a \rho_S a^\dagger - \frac{1}{2} \{ \rho_S, a a^\dagger \} \right) dt \right] dt \\ & + \kappa \left[\langle a_{\text{in}} a_{\text{in}}^\dagger \rangle \left(a^\dagger \rho_S a - \frac{1}{2} \{ \rho_S, a^\dagger a \} \right) dt \right] dt, \end{aligned} \quad (3.74)$$

where I denote $\rho_S = \rho_S(t)$ and the environment degrees of freedom are traced out. Here the topmost row corresponds to the isolated evolution of the density operator, and the next row, involving the commutators with the density operator, is related to the time evolution associated with the coupling to the environment. The terms proportional to

$a_{\text{in}}^\dagger a_{\text{in}}$ and $a_{\text{in}} a_{\text{in}}^\dagger$ describe dissipation whereas the terms with $a_{\text{in}}^{(\dagger)} a_{\text{in}}^{(\dagger)}$ are responsible of dephasing [36].

Suppose now that the environment is a bath with thermal noise. The following relations are then recovered [19]

$$\langle a_{\text{in}}^\dagger dt a_{\text{in}} dt \rangle = N dt, \quad (3.75a)$$

$$\langle a_{\text{in}} dt a_{\text{in}}^\dagger dt \rangle = (N + 1) dt, \quad (3.75b)$$

$$\langle a_{\text{in}} dt a_{\text{in}} dt \rangle = M dt, \quad (3.75c)$$

$$\langle a_{\text{in}} dt \rangle = \beta dt, \quad (3.75d)$$

where $0 \leq N \in \mathbb{R}$ and $M, \beta \in \mathbb{C}$ so that $|M|^2 \leq N(N + 1)$. If the system is in thermal equilibrium, $\beta = M = 0$ and $N = N_{\text{th}}$, where

$$N_{\text{th}}(\omega_n) = \left(e^{\frac{\omega_n}{k_b T}} - 1 \right)^{-1} \quad (3.76)$$

is the thermal population of the environment at temperature T .

Thus in thermal equilibrium, the Master equation of the linearly dissipative system is

$$\begin{aligned} \dot{\rho}_S = & -i [H_S, \rho_S] + N_{\text{th}} \kappa \left[a \rho_S a^\dagger - \frac{1}{2} \{ \rho_S, a a^\dagger \} \right] \\ & + (N_{\text{th}} + 1) \kappa \left[a^\dagger \rho_S a - \frac{1}{2} \{ \rho_S, a^\dagger a \} \right]. \end{aligned} \quad (3.77)$$

Notice that $N_{\text{th}} \rightarrow 0$ when $T \rightarrow 0$. Therefore, at zero temperature, the Master equation is

$$\dot{\rho}_S = -i [H_S, \rho_S] + \kappa a^\dagger \rho_S a - \frac{\kappa}{2} \{ \rho_S, a^\dagger a \}. \quad (3.78)$$

Nonlinear model Hamiltonian

The following model, depicting the coupling between a harmonic oscillator and a heat bath environment, can be used to describe both cavities and mechanical resonators. In the context of mechanical resonators, nonlinear dissipation and damping of micromechanical resonators have attracted a lot of attention in the last few years [20, 23, 37, 38], including a nonlinearity not explained by the Duffing response reported by Singh et al. [39]. Graphene resonators are also used in optomechanical systems and can exhibit large quality factors [40]. Better understanding of the dissipation phenomena of mechanical resonators (and cavities) may help us to improve the performance of optomechanical systems.

The system Hamiltonian is given by Eq. (2.3). The Hamiltonian of the environment of the harmonic oscillator is given in Eq. (3.9) as a set of bosonic modes each with a distinct frequency ω_n . The interaction between the system and the environment is modeled with the following Hamiltonian

$$H_I = i \sum_n g_n^L [c_n^\dagger a - c_n a^\dagger] + i \sum_n g_n^N [c_n^\dagger a^2 - c_n a^{\dagger 2}], \quad (4.1)$$

where g_n^L and g_n^N describe the strengths of the linear and nonlinear couplings between the system and the n th mode of the environment, respectively, and $c_n^{(\dagger)}$ and $a^{(\dagger)}$ are the annihilation (creation) operators of the environment and the system. Note that the first linear interaction term corresponds to Eq. (3.10) and the quantum Langevin equation resulting from this type of interaction is already discussed above.

The nonlinear interaction introduced in Eq. (4.1) represents one of the possible choices, arguably the simplest, allowing the introduction of a nonlinear system-environment coupling. On the one hand, I explore the consequences on the form of the QLE in the presence of this nonlinear system-environment coupling in Sec. 4.1. The QLE is then solved and the solutions are then compared to the case of bare linear coupling in Sec. 4.2. Additionally, Sec. 4.3 focuses on the ME of a nonlinearly dissipative harmonic oscillator.

A possible justification for the appearance of a nonlinear system-environment coupling is presented in Chap. 6 where the idea that two-level systems (TLS) can give rise to a nonlinear interaction between environment and cavity modes is introduced.

4.1 Derivation of the quantum Langevin equation

Let us derive the equation of motion of the system field operator a in presence of a system-environment coupling of the form given in Eq. (4.1). In analogy to what I do in Sec. 3.2, I employ input-output formalism to derive the QLE of the system. While I later focus on the case of a harmonic oscillator coupled to a bath, let us leave the system unspecified for the input-output formalism to achieve the general EOM using the coupling (4.1).

Consider a total Hamiltonian constituted by the Hamiltonians of the system, the environment, and the interaction between these two

$$\begin{aligned} H &= H_S + H_E + H_I \\ &= H_S + \sum_n \omega_n c_n^\dagger c_n + i \sum_n g_n^L [c_n^\dagger a - c_n a^\dagger] + i \sum_n g_n^N [c_n^\dagger a^2 - c_n a^{\dagger 2}], \end{aligned} \quad (4.2)$$

where $a^{(\dagger)}$ and $c_n^{(\dagger)}$ are the annihilation (creation) operators of the system and the n th environment mode, respectively, in the Heisenberg picture.

The Hamiltonian H represents the Hamiltonian of a closed system. Therefore writing the Heisenberg EOM using this total Hamiltonian is justified. The equation of motion for the n th annihilation field operator of the environment is

$$\dot{c}_n(t) = i[H, c_n] = -i\omega_n c_n + g_n^L a + g_n^N a^2. \quad (4.3)$$

This EOM can be solved, in analogy to the linear case, as

$$c_n(t) = e^{-i\omega_n(t-t_0)} c_n(t_0) + g_n^L \int_{t_0}^t e^{-i\omega_n(t-t')} a(t') dt' + g_n^N \int_{t_0}^t e^{-i\omega_n(t-t')} a^2(t') dt'. \quad (4.4)$$

Analogously, the EOM for a can be written as

$$\dot{a}(t) = i[H, a] = i[H_S, a] - \sum_n (g_n^L + 2g_n^N a^\dagger) c_n. \quad (4.5)$$

Like for the linear case in Sec. 3.2, in the following I make the simplifying assumption that the coupling constants g_n^L and g_n^N are independent of the frequency of the n th environment mode

$$(g_n^L)^2 = \frac{\kappa_L}{2\pi D}; \quad (g_n^N)^2 = \frac{\kappa_N}{2\pi D}, \quad (4.6)$$

where D is the density of states over the oscillatory modes and it is considered to be a positive constant. Recall that $n = \omega_n D = \omega_n \partial n / \partial \omega_n$. Note that here κ_L corresponds to κ in the purely linear context of definition (3.17).

With this approximation, I can plug the solution for c_n (4.4) back into the EOM for a (4.5)

$$\begin{aligned} \dot{a}(t) &= i[H_S, a] - \sqrt{\frac{1}{2\pi D}} (\sqrt{\kappa_L} + 2\sqrt{\kappa_N} a^\dagger) \sum_n e^{-i\omega_n(t-t_0)} c_n(t_0) \\ &\quad - \frac{1}{2\pi D} (\sqrt{\kappa_L} + 2\sqrt{\kappa_N} a^\dagger) \sqrt{\kappa_L} \int_{t_0}^t \sum_n e^{-i\omega_n(t-t')} a(t') dt' \\ &\quad - \frac{1}{2\pi D} (\sqrt{\kappa_L} + 2\sqrt{\kappa_N} a^\dagger) \sqrt{\kappa_N} \int_{t_0}^t \sum_n e^{-i\omega_n(t-t')} a^2(t') dt'. \end{aligned} \quad (4.7)$$

Considering the identity, see Appendix A,

$$\sum_n e^{-i\omega_n(t-t')} = 2\pi |D| \delta(t-t') \quad (4.8)$$

and defining, as in the linear case,

$$a_{\text{in}} = -\sqrt{\frac{1}{2\pi D}} \sum_n e^{-i\omega_n(t-t_0)} c_n(t_0), \quad (4.9)$$

I can write the final form of the quantum Langevin equation for a as

$$\dot{a}_t = i[H_S, a_t] - \frac{\kappa_L}{2} a_t - \kappa_N a_t^\dagger a_t^2 - \sqrt{\kappa_L \kappa_N} \left(a_t^\dagger a_t + \frac{1}{2} a_t^2 \right) + \sqrt{\kappa_L} a_{\text{in},t} + 2\sqrt{\kappa_N} a_t^\dagger a_{\text{in},t}, \quad (4.10)$$

where the terms resulting from the linear system-environment interaction are also explicitly written out. The explicit time dependence of the field operator a is expressed using subscripts for notational convenience, showing that the time evolution is local in time, i.e. Markovian, on the same argument as for the case of pure linear coupling. Here the commutator describes the time evolution generated by the isolated system.

In the limit $\kappa_N \rightarrow 0$ we can see the form of the QLE resulting from only the linear system-environment coupling, see Eq. (3.18).

4.2 Solving the nonlinear quantum Langevin equation

In this Section, I solve the quantum Langevin equation (4.10) up to linear order in fluctuations of a . The obtained results are compared to the case of solely linearly coupled cavity as formulated in Eq. (3.21).

If the system is described by a harmonic oscillator Hamiltonian $H_S = \omega_{\text{cav}} a^\dagger a$, as in the case of an optical or microwave resonant cavity, or for the approximate description of a mechanical oscillator, Eq. (4.10) can be written as

$$\dot{a} = -i\omega_{\text{cav}} a - \frac{\kappa_L}{2} a - \kappa_N a^\dagger a^2 - \sqrt{\kappa_L \kappa_N} \left(a^\dagger a + \frac{1}{2} a^2 \right) + \sqrt{\kappa_L} a_{\text{in}} + 2\sqrt{\kappa_N} a^\dagger a_{\text{in}}. \quad (4.11)$$

With a view to the application of this description of nonlinear couplings to experimentally relevant conditions which include, for instance, the physics of optomechanical systems, I linearize the field operator a like in the case of the full optomechanical system discussed in Sec. 3.3 so that $a_{(in)} = \alpha_{(in),t} + \delta a_{(in)}$ where $\alpha_t = |\alpha| e^{-i\omega_p(t-t_0)}$ is the average field amplitude of the cavity strongly pumped by the input field and δa is a small fluctuation around this point rotating at the angular frequency of the cavity. The components of the input field both rotate at the angular frequency of the pump, ω_p .

Using this decomposition and neglecting all the fluctuation terms of second or higher order, I arrive to the following form of the QLE

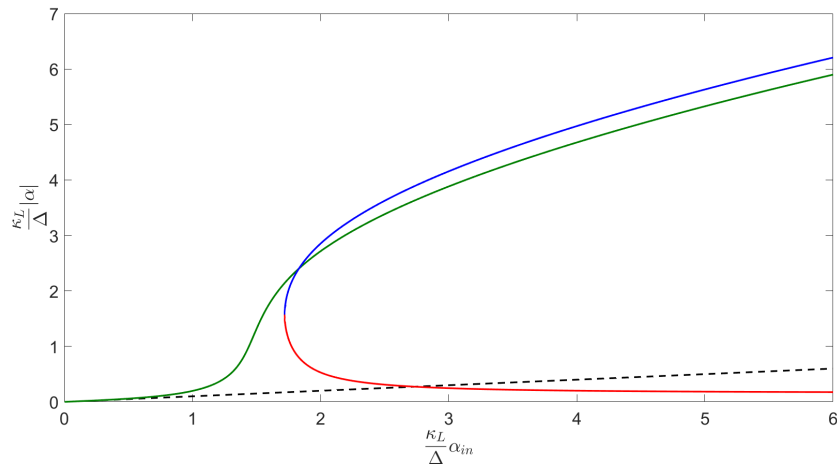
$$\begin{aligned} \delta \dot{a} = & i\Delta \alpha_t - \frac{\kappa_L}{2} \alpha_t - \kappa_N \alpha_t^* \alpha_t^2 - \sqrt{\kappa_L \kappa_N} \left(|\alpha|^2 + \frac{1}{2} \alpha_t^2 \right) + \sqrt{\kappa_L} \alpha_{\text{in},t} + 2\sqrt{\kappa_N} \alpha_t^* \alpha_{\text{in},t} \\ & - \left[i\omega_{\text{cav}} + \frac{\kappa_L}{2} + 2\kappa_N |\alpha|^2 + \sqrt{\kappa_L \kappa_N} (\alpha_t^* + \alpha_t) \right] \delta a \\ & - \left[\kappa_N \alpha_t^2 + \sqrt{\kappa_L \kappa_N} \alpha_t - 2\sqrt{\kappa_N} \alpha_{\text{in},t} \right] \delta a^\dagger + \left[\sqrt{\kappa_L} + 2\sqrt{\kappa_N} \alpha_t^* \right] \delta a_{\text{in}}, \end{aligned} \quad (4.12)$$

where the time derivative $\dot{\alpha}_t = -i\omega_p\alpha_t$, determined by the coherent pump, is utilized. $\Delta = \omega_p - \omega_{\text{cav}}$ is the detuning of the cavity.

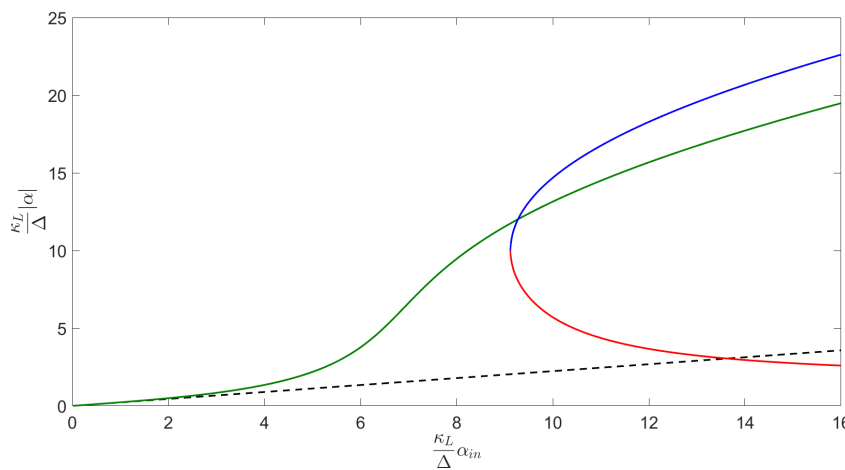
First, let us consider the zeroth order equation that determines the equilibrium solution, i.e. I neglect all the fluctuation terms of Eq. (4.12)

$$0 = i\Delta\alpha_t - \frac{\kappa_L}{2}\alpha_t - \kappa_N\alpha_t^*\alpha_t^2 - \sqrt{\kappa_L\kappa_N}\left(|\alpha|^2 + \frac{1}{2}\alpha_t^2\right) + \sqrt{\kappa_L}\alpha_{\text{in}} + 2\sqrt{\kappa_N}\alpha_t^*\alpha_{\text{in}}. \quad (4.13)$$

I fix $\alpha_{\text{in},t} = \alpha_{\text{in}} \in \mathbb{R}$ which corresponds to a specific choice of the time origin t_0 , and I solve for α_t . With this information $|\alpha|$ as a function of the input field can be constructed. Some numerical plots of $|\alpha|$ are shown in Figs. 7 and 8.



(a) $\kappa_L = 1 \cdot 10^{-2}\Delta$



(b) $\kappa_L = 5 \cdot 10^{-2}\Delta$

Figure 7: Numerical solutions of Eq. (4.13) for $|\alpha|$ as a function of the input field with different linear coupling strengths. Comparisons of the values of $|\alpha|$ between the results given by the bare linear coupling (dashed black), i.e. when $\kappa_N = 0$, and the full nonlinear model couplings (green, blue, red) are presented. The value of κ_L used to produce each plot is given below the respective figure. The detuning $\Delta = 1$ and the nonlinear coupling $\kappa_N = 1 \cdot 10^{-5}\Delta$ are kept constant.

Note that, due to energy minimization arguments, one has to consider that the physically acceptable solution is represented by the solution that minimizes $|\alpha|$. Furthermore, one

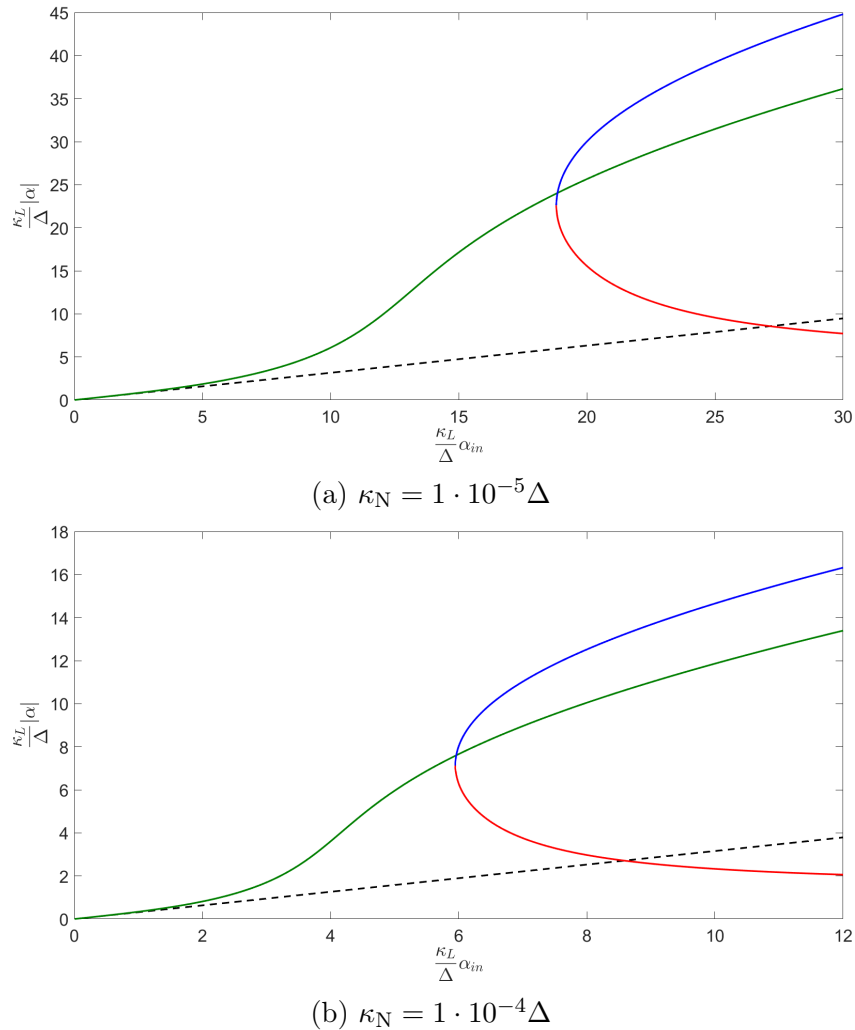


Figure 8: Numerical solutions of Eq. (4.13) for $|\alpha|$ as a function of the input field with different nonlinear coupling strengths. Comparisons of the values of $|\alpha|$ between the results given by the bare linear coupling (dashed black), i.e. when $\kappa_N = 0$, and the full nonlinear model couplings (green, blue, red) are presented. The values of κ_N are below the respective figures. The detuning $\Delta = 1$ and the linear coupling $\kappa_L = 0.1\Delta$ are kept constant.

can note that, contrary to the linear case, the α_{in} dependence of $|\alpha|$ is nonmonotonous; in particular for large enough values of a_{in} an increase of the input field leads to a decrease of the population of the harmonic oscillator. This behaviour is in contrast to the one encountered in the case of purely linear dissipation and speaks for the nonlinearity introduced by the extra nonlinear dissipation channel.

There are two distinct regions of the input field where there are either one or three solutions, respectively. For small values of α_{in} , the system behaves like in the case for which the linear dissipation only is present. However, for larger input fields, the nonlinear system behaviour starts to deviate from its linear counterpart and eventually three distinct solutions emerge. Figure 8 shows that by increasing the κ_N/κ_L ratio, the regime of input field values where the system behaves approximately linearly, decreases in size making the monotonically decreasing solution of $|\alpha|$ the physical solution starting from very small values of a_{in} .

Figures 7 and 8 show that regardless of the choice of the strength of the linear and nonlinear couplings, there is a threshold value of α_{in} where one of the metastable solutions becomes the stable physical solution. This new stable solution of $|\alpha|$ decreases monotonically with the increase of α_{in} making the behaviour of the cavity nonlinear for a strong input field. I consider the regime where $\kappa_L \gg \kappa_N$ and I take the lowest order approximation of Eq. (4.13) with respect to the nonlinear coupling granting me the value of the threshold in the regime $\Delta \gg \kappa_L$

$$\alpha_{\text{in}}^{\text{th}} = \frac{\sqrt{\kappa_L^2 + 4\Delta^2}}{4\sqrt{\kappa_N}}. \quad (4.14)$$

This choice is instrumental to the analysis that will be developed in the future, where the effect of nonlinear dissipation in optomechanical systems is considered. In the analysis of optomechanical systems, one is often lead to consider situations for which $|\Delta| \approx \omega_m$ which is implied in the regime in which the above threshold is derived, since usually $\omega_m \gg \kappa$. The full derivation of the threshold value is given in Appendix B. The approximate analytical values of the threshold are compared to some numerical calculations of the exact zeroth order approximation (4.13) in Fig. 9.

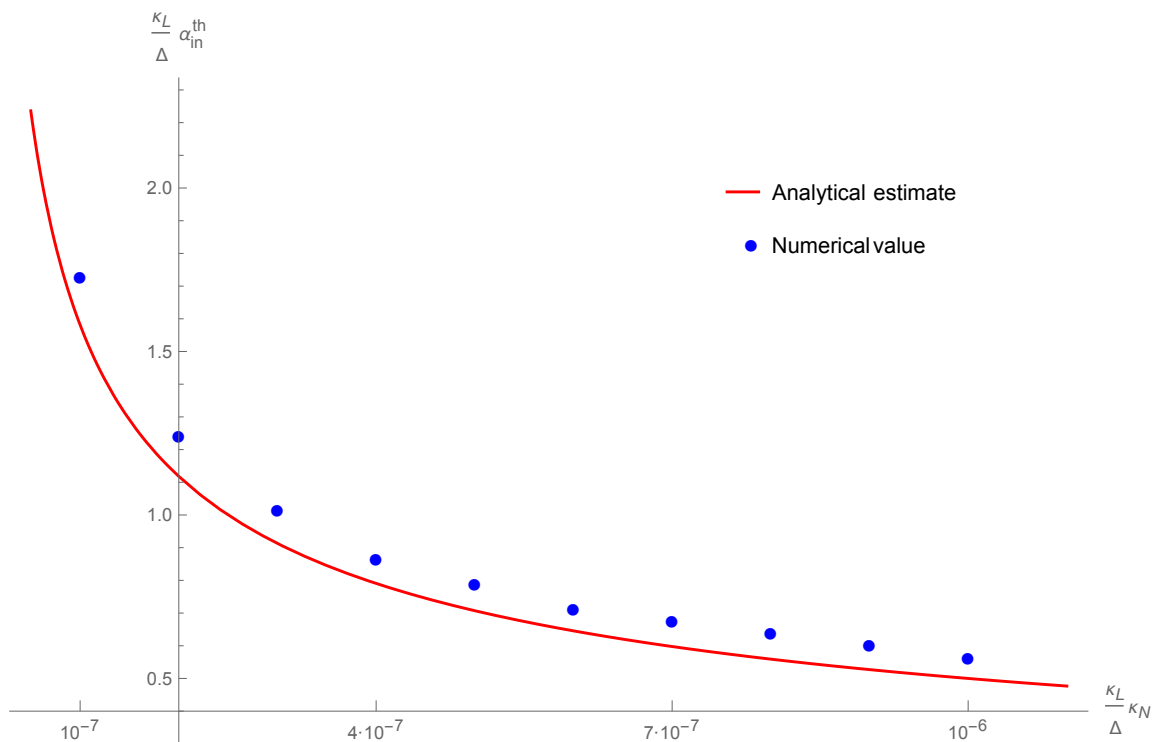


Figure 9: A comparison between the numerical solutions (blue dots) obtained from Eq. (4.13) and the analytical expression (red line) given by Eq. (4.14), respectively, of the threshold $\alpha_{\text{in}}^{\text{th}}$, where a metastable solution becomes the stable one, for different values of the nonlinear coupling constant κ_N . Here $\Delta = 1$ is kept constant as well as the linear coupling $\kappa_L = 1 \cdot 10^{-2} \Delta$ in order to be in the appropriate sideband regime for Eq. (4.14).

Now that the equilibrium solutions are derived, we examine the first order approximation around the point given by the zeroth order approximation. The EOM for δa is given by

Eq. (4.12)

$$\begin{aligned} \delta\dot{a} = & - \left[i\omega_{\text{cav}} + \frac{\kappa_{\text{L}}}{2} + 2\kappa_{\text{N}} |\alpha|^2 + \sqrt{\kappa_{\text{L}}\kappa_{\text{N}}} (\alpha_t^* + \alpha_t) \right] \delta a \\ & - \left[\kappa_{\text{N}}\alpha_t^2 + \sqrt{\kappa_{\text{L}}\kappa_{\text{N}}}\alpha_t - 2\sqrt{\kappa_{\text{N}}}\alpha_{\text{in}} \right] \delta a^\dagger + \left[\sqrt{\kappa_{\text{L}}} + 2\sqrt{\kappa_{\text{N}}}\alpha_t^* \right] \delta a_{\text{in}}. \end{aligned} \quad (4.15)$$

Note that by taking the Hermitian adjoint of both sides of Eq. (4.12), the EOM of δa^\dagger is obtained.

In the frame rotating at the cavity frequency, i.e. when $\omega_{\text{cav}} = 0$, we can write Eq. (4.15) in Fourier space as

$$\begin{aligned} \left[-i\omega + \frac{\kappa_{\text{L}}}{2} + 2\kappa_{\text{N}} |\alpha|^2 + \sqrt{\kappa_{\text{L}}\kappa_{\text{N}}} (\alpha_t^* + \alpha_t) \right] \delta a_\omega = & \left[-\kappa_{\text{N}}\alpha_t^2 - \sqrt{\kappa_{\text{L}}\kappa_{\text{N}}}\alpha_t + 2\sqrt{\kappa_{\text{N}}}\alpha_{\text{in}} \right] \delta a_{-\omega}^\dagger \\ & + \left[\sqrt{\kappa_{\text{L}}} + 2\sqrt{\kappa_{\text{N}}}\alpha_t^* \right] \delta a_{\text{in},\omega} \end{aligned} \quad (4.16)$$

and analogously for $\delta a_{-\omega}^\dagger$. With $\chi_c^{-1} = \left[-i\omega + \frac{\kappa_{\text{L}}}{2} + 2\kappa_{\text{N}} |\alpha|^2 + \sqrt{\kappa_{\text{L}}\kappa_{\text{N}}} (\alpha_t^* + \alpha_t) \right]$, $F = \left[\kappa_{\text{N}}\alpha_t^2 + \sqrt{\kappa_{\text{L}}\kappa_{\text{N}}}\alpha_t - 2\sqrt{\kappa_{\text{N}}}\alpha_{\text{in}} \right]$, and $\sqrt{\kappa} = \left[\sqrt{\kappa_{\text{L}}} + 2\sqrt{\kappa_{\text{N}}}\alpha_t^* \right]$ we get from Eq. (4.16)

$$\begin{pmatrix} \chi_c^{-1} & F \\ F^* & \chi_c^{-1} \end{pmatrix} \begin{pmatrix} \delta a_\omega \\ \delta a_{-\omega}^\dagger \end{pmatrix} = \begin{pmatrix} \sqrt{\kappa^*} \delta a_{\text{in},\omega} \\ \sqrt{\kappa} \delta a_{\text{in},-\omega}^\dagger \end{pmatrix}. \quad (4.17)$$

This can be solved to give

$$\begin{pmatrix} \delta a_\omega \\ \delta a_{-\omega}^\dagger \end{pmatrix} = \frac{\chi_c^2}{1 - |F|^2 \chi_c^2} \begin{pmatrix} \chi_c^{-1} & -F \\ -F^* & \chi_c^{-1} \end{pmatrix} \begin{pmatrix} \sqrt{\kappa^*} \delta a_{\text{in},\omega} \\ \sqrt{\kappa} \delta a_{\text{in},-\omega}^\dagger \end{pmatrix}. \quad (4.18)$$

Now that the fluctuations around the equilibrium solution are known, one can consider the uncertainty related to measurements performed on the system. In the quantum limit, a measurement of an observable always has some intrinsic uncertainty related to the measured observable and some other noncommuting observable. The most well known example is the Heisenberg uncertainty of position and momentum $\Delta x \Delta p \geq \hbar/2$ [34]. The following discussion on quantum uncertainty and quantum measurements follows an extensive review of the subject by Clerk et al. [13].

The noise spectral density of a quantum mechanical operator O describes the intrinsic uncertainty present in the measurement at a given frequency ω . Consider, for instance, an optomechanical system where one tries to measure the displacement of a mechanical resonator using an optical cavity. A change in position can be measured by observing the phase shift of the light in the cavity resulting from the change in the width of the cavity. The measurement of the phase has some uncertainty due to the imprecision of the position of the mirrors. Additionally photons transfer momentum to the mirrors causing backaction noise. These two noise sources are intrinsic properties of cavity measurements. When a mechanical oscillator is coupled with the cavity in order to measure its position, the momentum transferred by photons to the mirrors also change the momentum of the resonator, thus causing additional uncertainty.

The noise spectral density can be defined as

$$S_{OO}(\omega) = \int_{-\infty}^{\infty} dt e^{i\omega t} \langle O(t) O(0) \rangle, \quad (4.19)$$

i.e. it is the Fourier transform of the quantum autocorrelation function of operator O . Here the angular brackets denote the quantum statistical average. Note that quantum mechanical operators $O(t_1)$ and $O(t_2)$ do not necessarily commute at different times $t_1 \neq t_2$, and therefore the quantum spectral density is asymmetric in frequency and can be complex valued. Classically this cannot happen since classical variables, even if defined at different times, commute. The spectral density can be decomposed into parts that are symmetric and asymmetric in frequency. The symmetric part is analogous to classical noise and is given by

$$\bar{S}_{OO}(\omega) = \frac{1}{2} [S_{OO}(\omega) + S_{OO}(-\omega)] = \frac{1}{2} \int_{-\infty}^{\infty} dt e^{i\omega t} \langle \{O(t), O(0)\} \rangle, \quad (4.20)$$

where the curly brackets denote an anticommutator.

Now the symmetric spectral density characterizing the noise at a certain frequency can be identified as $\delta a_{\omega}^{\dagger} \delta a_{\omega} + \delta a_{-\omega}^{\dagger} \delta a_{-\omega}$, and it can be plotted as a function of the frequency ω , see Fig. 10. I consider small enough values of $|\alpha|$ so that $|\alpha|$ is still in the linear regime as a function of the input field, see Fig. 7, i.e. it obeys the relation

$$|\alpha| = \sqrt{\frac{\kappa_L}{\frac{\kappa_L^2}{4} + \Delta^2}} \alpha_{\text{in}}. \quad (4.21)$$

Also only the sideband regime, where the threshold value $\alpha_{\text{in}}^{\text{th}}$ (4.14) is valid, is considered since it is the one that is best understood.

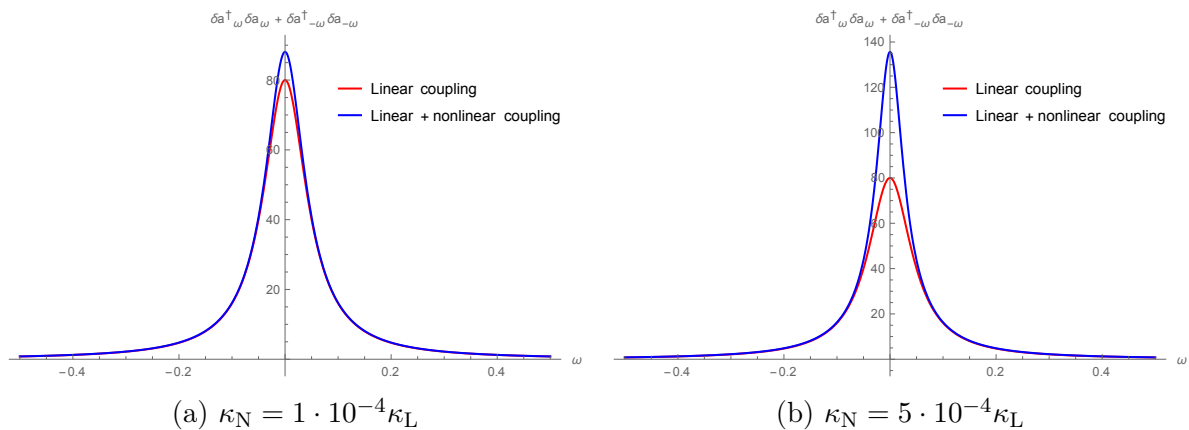


Figure 10: The responses $\delta a_{\omega}^{\dagger} \delta a_{\omega} + \delta a_{-\omega}^{\dagger} \delta a_{-\omega}$ of the cavity coupled linearly (red), Eq. (3.10) and nonlinearly (blue), Eq. (4.1), to the environment. For both figures the used parameters are $\Delta = 1$, $\kappa_L = 0.1\Delta$ and $\alpha_t = 0.5$. The values of κ_N used in each plot are given by the respective figures.

The peak of the measurement noise is centered at the fundamental frequency of the cavity for both the linear ($\kappa_N = 0$) and the nonlinear ($\kappa_N > 0$) couplings. When the nonlinear coupling is present, the uncertainty of a measurement is higher compared to the linear interaction. Additionally we see that an increase in the strength of the nonlinear coupling leads to a higher maximum uncertainty. However, the uncertainty distribution is not widened by the increase of κ_N meaning that the linewidth of the uncertainty distribution decreases. Thus the error in the measurement, although always present and larger in value

compared to the linear case, is better localized in the frequency space when the nonlinear interaction is considered.

Recall that α_t rotates at the frequency of the pump ω_p . For the linear coupling alone the spectral density does not depend on α_t which can be seen from (4.18) by setting $\kappa_N \rightarrow 0$. However, this is not the case when the nonlinear coupling differs from zero. Figure 11 shows that for the nonlinear case the spectral density is affected by the choice of the phase of α_t . In the regime $\Delta \gg \kappa_L \gg \kappa_N$, the reversal of phase from α_t to $-\alpha_t$ makes the peak of the uncertainty distribution even higher. This effect is more noticeable for larger values of κ_N .

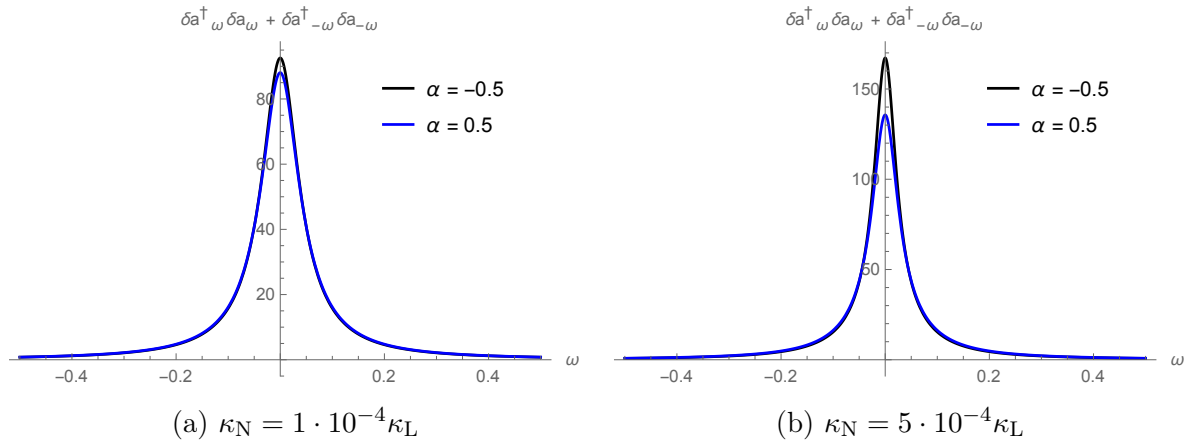


Figure 11: The responses $\delta a_{\omega}^{\dagger} \delta a_{\omega} + \delta a_{-\omega}^{\dagger} \delta a_{-\omega}$ of the cavity coupled nonlinearly to the environment with the Hamiltonian (4.1) for opposite phases of α , more precisely $\alpha_t = -0.5$ (black) and $\alpha_t = 0.5$ (blue). For both figures $\Delta = 1$ and $\kappa_L = 0.1\Delta$. The values of κ_N are denoted under the respective figures.

4.3 Master equation for the nonlinearly dissipative harmonic oscillator

Let us determine the Master equation of a nonlinearly dissipative system described by the QLE (4.10). Recall from the case of linear dissipation the form of the EOM (3.67) for the system operator a . The following form of L is taken as an ansatz

$$L = \left[\sqrt{\kappa_L} \left(a_0^{\dagger} a_{\text{in}} - a_0 a_{\text{in}}^{\dagger} \right) + \sqrt{\kappa_N} \left(a_0^{\dagger 2} a_{\text{in}} - a_0^2 a_{\text{in}}^{\dagger} \right) \right] dB. \quad (4.22)$$

as opposed to the linear case where only the first term is present.

The input terms of the QLE (4.10) are obtained from the following commutator

$$[a_0, L] dB = \left(\sqrt{\kappa_L} a_{\text{in}} + 2\sqrt{\kappa_N} a_0^{\dagger} a_{\text{in}} \right) dt. \quad (4.23)$$

The other terms of the ME are

$$\begin{aligned}
\left[-La_0L + \frac{1}{2} \{a_0, L^2\} \right] dt &= \left\{ -\frac{\kappa_L}{2} a_0 [a_{\text{in}}, a_{\text{in}}^\dagger] dt - \kappa_N a_0^\dagger a_0^2 [a_{\text{in}}, a_{\text{in}}^\dagger] dt \right. \\
&\quad - \sqrt{\kappa_L \kappa_N} \left(a_0^\dagger a_0 + \frac{1}{2} a_0^2 \right) [a_{\text{in}}, a_{\text{in}}^\dagger] dt \\
&\quad \left. + (2\kappa_N a_0 + \sqrt{\kappa_L \kappa_N}) a_{\text{in}}^\dagger a_{\text{in}} dt \right\} dt \\
&= -\frac{\kappa_L}{2} a_0 dt - \kappa_N a_0^\dagger a_0^2 dt \\
&\quad - \sqrt{\kappa_L \kappa_N} \left(a_0^\dagger a_0 + \frac{1}{2} a_0^2 \right) dt \\
&\quad + (2\kappa_N a_0 + \sqrt{\kappa_L \kappa_N}) a_{\text{in}}^\dagger a_{\text{in}} dt^2,
\end{aligned} \tag{4.24}$$

where the commutation relation (3.72) is used.

Combining Eqs. (4.23) and (4.24) shows that

$$\begin{aligned}
a(dt) &= \left[i[H_S, a_0] - \frac{\kappa_L}{2} a_0 - \kappa_N a_0^\dagger a_0^2 - \sqrt{\kappa_L \kappa_N} \left(a_0^\dagger + \frac{1}{2} a_0^2 \right) \right. \\
&\quad \left. + \sqrt{\kappa_L} a_{\text{in}} + 2\sqrt{\kappa_N} a_0^\dagger a_{\text{in}} \right] dt + (2\kappa_N a_0 + \sqrt{\kappa_L \kappa_N}) a_{\text{in}}^\dagger a_{\text{in}} dt^2.
\end{aligned} \tag{4.25}$$

Using Eqs. (3.75a) and (3.76) one can see that Eq. (4.25) approaches the QLE (4.10) for an environment in a thermal equilibrium in the limit $T \rightarrow 0$. However, let us not go to that limit as of yet, but instead write the general Master equation given by the ansatz (4.22)

$$\begin{aligned}
\rho_S(dt) &= \rho_S - i[H_S, \rho_S] dt \\
&\quad - \sqrt{\kappa_L} [\rho_S, a^\dagger] \langle a_{\text{in}} \rangle dt + \sqrt{\kappa_L} [\rho_S, a] \langle a_{\text{in}}^\dagger \rangle dt \\
&\quad - \sqrt{\kappa_N} [\rho_S, a^{\dagger 2}] \langle a_{\text{in}} \rangle dt + \sqrt{\kappa_N} [\rho_S, a^2] \langle a_{\text{in}}^\dagger \rangle dt \\
&\quad - \left[\langle a_{\text{in}} a_{\text{in}} \rangle \left(\kappa_L a^\dagger \rho_S a^\dagger + \kappa_N a^{\dagger 2} \rho_S a^{\dagger 2} + \sqrt{\kappa_L \kappa_N} a^\dagger \rho_S a^{\dagger 2} + \sqrt{\kappa_L \kappa_N} a^{\dagger 2} \rho_S a \right) \right. \\
&\quad \quad \left. - \frac{1}{2} \{ \rho_S, \kappa_L a^{\dagger 2} + \kappa_N a^{\dagger 4} + 2\sqrt{\kappa_L \kappa_N} a^{\dagger 3} \} \right] dt \\
&\quad - \left[\langle a_{\text{in}}^\dagger a_{\text{in}}^\dagger \rangle \left(\kappa_L a \rho_S a + \kappa_N a^2 \rho_S a^2 + \sqrt{\kappa_L \kappa_N} a \rho_S a^2 + \sqrt{\kappa_L \kappa_N} a^2 \rho_S a \right) \right. \\
&\quad \quad \left. - \frac{1}{2} \{ \rho_S, \kappa_L a^2 + \kappa_N a^4 + 2\sqrt{\kappa_L \kappa_N} a^3 \} \right] dt \\
&\quad + \left[\langle a_{\text{in}}^\dagger a_{\text{in}} \rangle \left(\kappa_L a \rho_S a^\dagger + \kappa_N a^2 \rho_S a^{\dagger 2} + \sqrt{\kappa_L \kappa_N} a \rho_S a^{\dagger 2} + \sqrt{\kappa_L \kappa_N} a^2 \rho_S a^\dagger \right) \right. \\
&\quad \quad \left. - \frac{1}{2} \{ \rho_S, \kappa_L a a^\dagger + \kappa_N a^2 a^{\dagger 2} + \sqrt{\kappa_L \kappa_N} a^2 a^\dagger + \sqrt{\kappa_L \kappa_N} a a^{\dagger 2} \} \right] dt \\
&\quad + \left[\langle a_{\text{in}} a_{\text{in}}^\dagger \rangle \left(\kappa_L a^\dagger \rho_S a + \kappa_N a^{\dagger 2} \rho_S a^2 + \sqrt{\kappa_L \kappa_N} a^\dagger \rho_S a^2 + \sqrt{\kappa_L \kappa_N} a^{\dagger 2} \rho_S a \right) \right. \\
&\quad \quad \left. - \frac{1}{2} \{ \rho_S, \kappa_L a^\dagger a + \kappa_N a^{\dagger 2} a^2 + \sqrt{\kappa_L \kappa_N} a^\dagger a^2 + \sqrt{\kappa_L \kappa_N} a^{\dagger 2} a \} \right] dt,
\end{aligned} \tag{4.26}$$

where I denote $\rho_S = \rho_S(0)$ and $a = a_0$. Note that at finite temperature this is an approximate description of the dynamics of the system, since the QLE (4.10) is not

satisfied exactly using the ansatz (4.22) even though the chosen form of L is the only anti-Hermitian operator that generates the correct input field terms.

Using Eqs. (3.75a)–(3.75d), at thermal equilibrium the Master equation of the nonlinearly dissipative system is

$$\begin{aligned}
\dot{\rho}_S = & -i[H_S, \rho_S] \\
& + N_{\text{th}} \left[\kappa_L a \rho_S a^\dagger + \kappa_N a^2 \rho_S a^{\dagger 2} + \sqrt{\kappa_L \kappa_N} a \rho_S a^{\dagger 2} + \sqrt{\kappa_L \kappa_N} a^2 \rho_S a^\dagger \right. \\
& \quad \left. - \frac{1}{2} \left\{ \rho_S, \kappa_L a a^\dagger + \kappa_N a^2 a^{\dagger 2} + \sqrt{\kappa_L \kappa_N} a^2 a^\dagger + \sqrt{\kappa_L \kappa_N} a a^{\dagger 2} \right\} \right] \\
& + (N_{\text{th}} + 1) \left[\kappa_L a^\dagger \rho_S a + \kappa_N a^{\dagger 2} \rho_S a^2 + \sqrt{\kappa_L \kappa_N} a^\dagger \rho_S a^2 + \sqrt{\kappa_L \kappa_N} a^{\dagger 2} \rho_S a \right. \\
& \quad \left. - \frac{1}{2} \left\{ \rho_S, \kappa_L a^\dagger a + \kappa_N a^{\dagger 2} a^2 + \sqrt{\kappa_L \kappa_N} a^\dagger a^2 + \sqrt{\kappa_L \kappa_N} a^{\dagger 2} a \right\} \right].
\end{aligned} \tag{4.27}$$

At zero temperature, the ME of the nonlinearly dissipative system has the following form

$$\begin{aligned}
\dot{\rho}_S = & -i[H_S, \rho_S] + \kappa_L a^\dagger \rho_S a + \kappa_N a^{\dagger 2} \rho_S a^2 + \sqrt{\kappa_L \kappa_N} a^\dagger \rho_S a^2 + \sqrt{\kappa_L \kappa_N} a^{\dagger 2} \rho_S a \\
& - \frac{1}{2} \left\{ \rho_S, \kappa_L a^\dagger a + \kappa_N a^{\dagger 2} a^2 + \sqrt{\kappa_L \kappa_N} a^\dagger a^2 + \sqrt{\kappa_L \kappa_N} a^{\dagger 2} a \right\}.
\end{aligned} \tag{4.28}$$

Notice that this ME is not in the Lindblad form (3.62) even though the system is imposed to be Markovian. This is due to the nonlinear system-environment interaction and the choice of the form of the zeroth Kraus operator (3.65) to correctly create the input dynamics of the QLE. However, a non-Lindblad form ME of the system (S) can be formulated in the Lindblad form with the help of some ancillary environment (A) so that the dynamics of the combined S–A system can be described in the Lindblad form [41].

Review of two-level systems

This Chapter serves as a general introduction to two-level systems, and aims to illustrate how interactions with TLSs can be modeled, e.g. when a TLS is under stress.

5.1 Algebra of two-level systems

TLSs can be found in various physical systems such as tunneling atoms [42] that are encountered, e.g. in amorphous glasses [43]. Another example of TLSs are dangling bonds that are atoms, immobilized e.g. in a solid, that have an unpaired valence electron. Their chemical behaviour is similar to free radicals. Dangling bonds can be found, for instance, on silicon surfaces [44, 45]. Also nanomechanical beams can act as TLSs as shown by Faust et al. [46] in their experiment, where a silicon nitride beam having two orthogonal vibrational modes is driven by radio frequency signals. A typical textbook example of a solvable TLS is a spin- $\frac{1}{2}$ system, such as an electron, in an external magnetic field [47].

Formally the Hamiltonian of a TLS can be expressed on a two-dimensional Hilbert space spanned by two states, say $|a\rangle$ and $|b\rangle$, as a linear combination of the Pauli matrices

$$\sigma_x = \begin{pmatrix} 0 & 1 \\ 1 & 0 \end{pmatrix}, \quad \sigma_y = \begin{pmatrix} 0 & -i \\ i & 0 \end{pmatrix}, \quad \sigma_z = \begin{pmatrix} 1 & 0 \\ 0 & -1 \end{pmatrix} \quad (5.1)$$

that obey the commutation relation

$$[\sigma_j, \sigma_k] = 2i\varepsilon_{jkl}\sigma_l, \quad (5.2)$$

and operate on the two states of the TLS in the following way

$$\begin{aligned} \sigma_x |a\rangle &= |b\rangle, & \sigma_y |a\rangle &= i|b\rangle, & \sigma_z |a\rangle &= |a\rangle, \\ \sigma_x |b\rangle &= |a\rangle, & \sigma_y |b\rangle &= -i|a\rangle, & \sigma_z |b\rangle &= -|b\rangle. \end{aligned} \quad (5.3)$$

Especially one can see that the state of the TLS can be flipped using the following ladder operators

$$\sigma_- |a\rangle = \frac{1}{2}(\sigma_x - i\sigma_y) |a\rangle = |b\rangle, \quad \sigma_+ |b\rangle = \frac{1}{2}(\sigma_x + i\sigma_y) |b\rangle = |a\rangle. \quad (5.4)$$

Alternatively, one can express the TLS in the Schwinger representation using the bosonic annihilation (creation) operators $d_{a/b}^{(\dagger)}$ of the a/b state of the TLS. The number operators of the two states are

$$n_a = d_a^\dagger d_a \quad n_b = d_b^\dagger d_b. \quad (5.5)$$

Thus the spin operators can be defined

$$\begin{aligned}
 J_x &= d_a^\dagger d_b + d_b^\dagger d_a, \\
 J_y &= i \left(d_b^\dagger d_a - d_a^\dagger d_b \right), \\
 J_z &= n_a - n_b, \\
 J_+ &= d_a^\dagger d_b, \\
 J_- &= d_b^\dagger d_a.
 \end{aligned}
 \tag{5.6}$$

One can easily check that the Eq. (5.6) is in agreement with definitions (5.2)–(5.4).

5.2 Modeling two-level systems and the interaction with them

Large dielectric losses in superconducting quantum bits have been shown to be a major source of decoherence for these qubits in low temperatures and weak driving voltages [48]. This decoherence is proposed to be due to a coupling to a bath of two-level systems that can interact with the surrounding electric field using their dipole moments. The two-level systems get saturated in higher temperatures and voltages thus making the effect less relevant in this regime. Similarly TLSs are used to explain the excess dielectric loss in various amorphous materials [49].

In Chap. 6, I derive nonlinear dissipation effects of a harmonic oscillator as a result of the mediation of the oscillator/environment by an ensemble of two-level systems. This derivation represents a general justification of the nonlinear interaction Hamiltonian (4.1), but it is not an exact derivation.

In the context of superconducting QED and nanomechanical systems, a TLS can be represented by a double well potential [43, 50, 51], see Fig. 12, in which a particle is allowed to tunnel between two local energy minima with energy separation Δ_0 through a barrier of height V and thickness d . The energy separation of the two states is given by $\Delta_0 = \omega e^{-\lambda}$, where ω is the frequency of the tunneling particle, and the tunneling parameter λ is given by the barrier properties so that $\lambda = d\sqrt{2mV}$, where m is the mass of the tunneling particle. Such a tunneling particle can be, for instance, a certain mechanical mode with effective mass m if one considers a mechanical system or a charged ion moving between two energy minima.

Let us focus on a TLS under tension, and consider that mechanical and dielectric TLSs can be handled analogously [50]. On the one hand, a mechanical TLS can be, for instance, a mechanical system that has two possible vibrational modes [46]. On the other hand, dielectric materials are insulators that can be polarized by applying an electric field. For example, dielectric TLSs can exist in glasses where, due to their amorphous nature, energy minima with some energy separation are present and they can be occupied by ions [43].

An external strain field mediated by phonons, in the mechanical (acoustic) case, or by an electric field, in the dielectric case, modifies the shape of the wells. The external strain deforms the environment of the tunneling particle, altering the energy splitting Δ between the two wells. In this case the energies of the two eigenstates of the TLS differ by $E = \sqrt{\Delta_0^2 + \Delta^2}$. The mechanical deformation potentials and dielectric dipole moments,

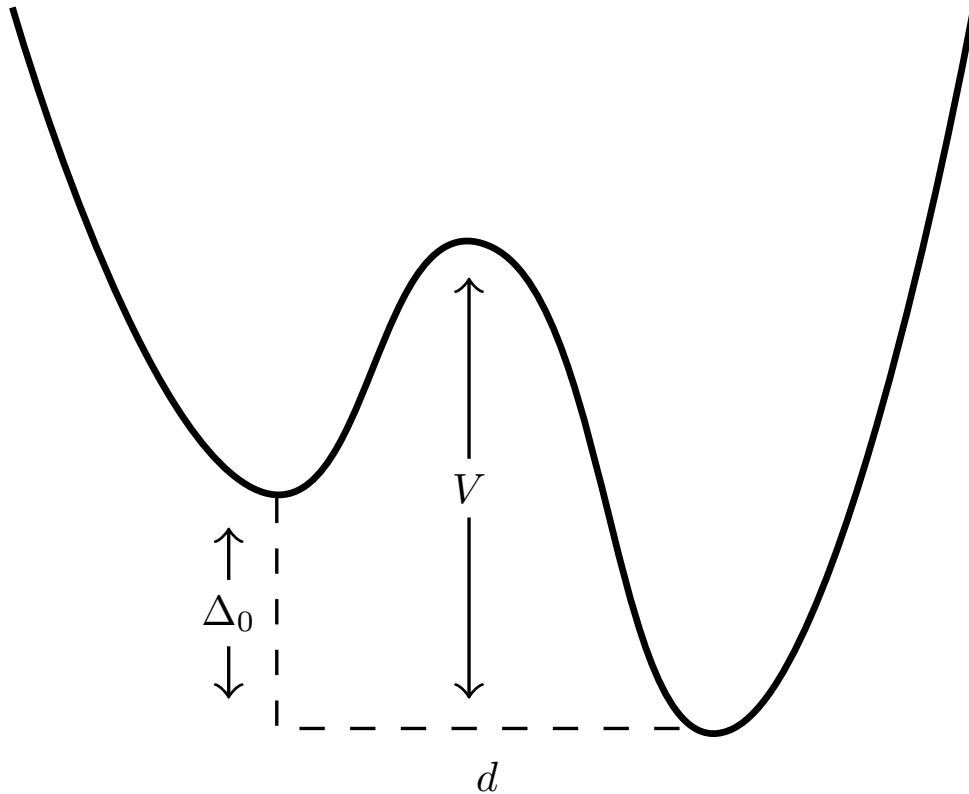


Figure 12: Schematic of the tunneling model of a two-level system. The TLS is formed using a double well potential whose two local energy minima are separated by a potential well of height V and thickness d . The energy difference of the minima is Δ_0 .

D , D' and μ , μ' , respectively, can be expressed as [50]

$$\begin{aligned} D &= \frac{2\gamma\Delta}{E}, \\ D' &= \frac{2\gamma\Delta_0}{E}, \\ \mu &= \frac{2p\Delta}{E}, \\ \mu' &= \frac{2p\Delta_0}{E}. \end{aligned} \tag{5.7}$$

The parameters γ and p tell how much the TLS is deformed under the mechanical strain field $|\vec{\epsilon}|$ or the electric field $|\vec{E}|$, respectively, so that $2\gamma = d\Delta/d|\vec{\epsilon}|$ and $2p = d\Delta/d|\vec{E}|$. Note that these quantities are determined in the direction of the applied field. The Hamiltonian of a dielectric TLS under electromagnetic strain can be written as [50]

$$H_{\text{TLS}} = \frac{E}{2}\sigma_z - \frac{1}{2}(\mu\sigma_z + 2\mu'\sigma_x)|\vec{E}|, \tag{5.8}$$

and its mechanical analog with the following replacements: $|\vec{E}| \rightarrow |\vec{\epsilon}|$, $\mu \rightarrow D$, and $\mu' \rightarrow D'$.

To model the dissipation of a two-level system, the *spin-boson model* is often used [51, 52]. In the spin-boson model, the two-level system is embedded in a heat bath described by

a set of bosonic harmonic oscillators given by the familiar Hamiltonian H_E (3.9). Also the environment is coupled to the TLS by σ_z so that, in its second quantized form, the spin-boson model Hamiltonian is

$$H_{S-B} = H_{\text{TLS}} + H_E + \sigma_z \sum_j g_j (c_j + c_j^\dagger), \quad (5.9)$$

where g_j is the coupling strength and $(c_j + c_j^\dagger)$ the displacement associated with the j th oscillator in the environment. In general, the dynamics that follow from this type of coupling are non-Markovian [53]. Extensions of this model are also explored in the literature, e.g. the inclusion of the nonlinear coupling $\sigma_z \sum_{j,k} g_j g_k (c_j + c_j^\dagger) (c_k + c_k^\dagger)$ between the TLS and the environment [51, 52]. Relaxation and dephasing times of the TLS can be calculated for various dissipation schemes for the standard spin-boson model (5.9) and also for the quadratic coupling version of the model [52].

Derivation of nonlinear phenomena

The following derivation can be seen as a loose justification for the nonlinear model Hamiltonian (4.2) even though here I specifically focus on an optical cavity instead of a nonspecific harmonic oscillator. We propose a general model that takes the advantage of coupling the system and environment via two-level systems to explain the manifestation of nonlinearities in the optical framework of optomechanics.

An effective model in a certain subspace of the total Hilbert space can be obtained from the full Hamiltonian of the tripartite system by applying a so-called Schrieffer-Wolff transformation. The model that is derived through this procedure can be, to some extent, approximated to contain terms similar to the simple nonlinear model Hamiltonian (4.2) although several other nonlinear interactions appear as well.

6.1 Interaction between light and matter

The standard QED formulation that is used here closely follows the formulation presented in the book *Quantum optics* by Walls and Milburn [36]. The minimum substitution Hamiltonian describing the interaction between an electron and an electromagnetic field, light in the case of an optical cavity, is of the form [36]

$$H = \frac{1}{2m} (\vec{p} - e\vec{A})^2 + eV(\vec{x}) + H_{\text{field}}, \quad (6.1)$$

where \vec{A} is the vector potential of the EM field, \vec{p} , m , and e are the momentum, the mass, and the charge of the electron, respectively, and $V(\vec{x})$ is a position-dependent potential that the electron feels. The vector potential of the EM field has a general second quantized form

$$\vec{A} = \sum_{m,n} \sqrt{\frac{1}{2\epsilon_0\omega_n}} e_{m,n} [u_n(\vec{x}) b_n + u_n^*(\vec{x}) b_n^\dagger], \quad (6.2)$$

where $e_{m,n}$ is the polarization vector, ϵ_0 the vacuum permittivity, ω_n the frequency corresponding to the n th field mode, and $b_n^{(\dagger)}$ the second quantized annihilation (creation) field operator of the n th mode of the EM field. For a box-shaped space, of volume V , the mode functions $u_n(\vec{x})$ take the form $u_n(\vec{x}) = V^{-\frac{1}{2}} e^{i\vec{k}_n \cdot \vec{x}}$ and from now on I denote $\xi_n = (2\epsilon_0\omega_n V)^{-\frac{1}{2}}$. For the majority of this Section, I use the vector potential of only one mode, denoted by b , not to be mistaken for the field operator of the mechanical part of an optomechanical system above. The results obtained for this single mode can easily be modified to describe multiple modes, namely the cavity and the environment, whose field operators are denoted by a and c_n , respectively.

The second quantized formulation of the minimum substitution Hamiltonian (6.1) is

$$H = H_{\text{el}} + H_{\text{int}} + H_{\text{field}}, \quad (6.3)$$

where the electron and EM field Hamiltonians are, respectively,

$$H_{\text{el}} = \int \hat{\psi}^\dagger(\vec{x}) \left(\frac{p^2}{2m} + eV(\vec{x}) \right) \hat{\psi}(\vec{x}) d\vec{x} = \sum_j E_j d_j^\dagger d_j, \quad (6.4)$$

$$H_{\text{field}} = \sum_n \omega_n b_n^\dagger b_n. \quad (6.5)$$

Here the second quantized electron field operators $\hat{\psi}(\vec{x})$ can be written in terms of unperturbed single particle states $\phi_j(\vec{x})$ and fermionic annihilation (creation) operators $d_j^{(\dagger)}$ so that $\hat{\psi}(\vec{x}) = \sum_j d_j \phi_j(\vec{x})$. The orthonormality of the functions $\phi_j(\vec{x})$ is the cause of the rightmost equality of Eq. (6.4), and $H_e \phi_j(\vec{x}) = \left(\frac{p^2}{2m} + eV(\vec{x}) \right) \phi_j(\vec{x}) = E_j \phi_j(\vec{x})$. The field operators of the electron obey the common fermionic anticommutation conventions.

The interaction part of the total Hamiltonian can be written in terms of a linear interaction between the charged particle and the EM field

$$H_{\text{int},1} = -\frac{e}{2m} \int \hat{\psi}^\dagger(\vec{x}) \left(\vec{A} \cdot \vec{p} + \vec{p} \cdot \vec{A} \right) \hat{\psi}(\vec{x}) d\vec{x} \quad (6.6)$$

and a quadratic interaction, given that the EM field is strong

$$H_{\text{int},2} = \frac{e^2}{2m} \int \hat{\psi}^\dagger(\vec{x}) \vec{A}^2 \hat{\psi}(\vec{x}) d\vec{x}. \quad (6.7)$$

Let us first focus on the linear interaction whose Hamiltonian can be explicitly written as

$$H_{\text{int},1} = -\frac{e}{2m} \sum_{j,k,\alpha} \sqrt{\frac{1}{2\epsilon_0\omega_\alpha}} d_j^\dagger d_k \int \phi_j^*(\vec{x}) \left[(b_\alpha \vec{u}_\alpha(\vec{x}) + b_\alpha^\dagger \vec{u}_\alpha^*(\vec{x})) \cdot \vec{p} \right. \\ \left. + \vec{p} \cdot (b_\alpha \vec{u}_\alpha(\vec{x}) + b_\alpha^\dagger \vec{u}_\alpha^*(\vec{x})) \right] \phi_k(\vec{x}) d\vec{x} \quad (6.8)$$

In this derivation, I am focusing on EM fields in the optical regime, and therefore the wavelength of the radiation, $\lambda_{\text{photon}} = 2\pi/|\vec{k}|$, is much longer than the characteristic size of the volume where the electrons are confined, e.g. an atom. This entails that $\vec{u}_\alpha(\vec{x})$ varies in a larger lengthscale than the electron wavefunctions $\phi_k(\vec{x})$, and therefore the dipole approximation is valid, allowing us to approximate

$$H_{\text{int},1} = -\frac{e}{m} \sum_{j,k,\alpha} \xi_\alpha d_j^\dagger d_k \left(b_\alpha e^{i\vec{k}_\alpha \cdot \vec{x}_0} + b_\alpha^\dagger e^{-i\vec{k}_\alpha \cdot \vec{x}_0} \right) \int \phi_j^*(\vec{x}) p \phi_k(\vec{x}) d\vec{x}. \quad (6.9)$$

Looking at the second quantized electron Hamiltonian (6.4), it can immediately be seen that, except for the momentum part, everything commutes with \vec{x} . This can be utilized together with the commutation relation, $[p^2, x] = -i2p$

$$\int \phi_j^*(\vec{x}) p \phi_k(\vec{x}) d\vec{x} = im \int \phi_j^*(\vec{x}) [H_e, \vec{x}] \phi_k(\vec{x}) d\vec{x} = im v_{j,k} \int \phi_j^*(\vec{x}) \vec{x} \phi_k(\vec{x}) d\vec{x}, \quad (6.10)$$

where $v_{j,k} = E_j - E_k$ is the difference of eigenenergies of the j th and k th electron states. The rightmost equality comes from the stationary Schrödinger equation $H_e \phi_n(\vec{x}) = E_n \phi_n(\vec{x})$.

Let us define the coupling strength for the linear interaction term as

$$g_{jk\alpha} = -iev_{j,k}\xi_\alpha e^{i\vec{k}_\alpha \cdot \vec{x}_0} \int \phi_j^*(\vec{x}) \vec{x} \phi_k(\vec{x}) d\vec{x} \quad (6.11)$$

and choose the phase of $g_{jk\alpha}$ so that the coupling constant is real valued. The linear interaction Hamiltonian can be written as

$$H_{\text{int},1} = \sum_{j,k,\alpha} d_j^\dagger d_k g_{jk\alpha} (b_\alpha + b_\alpha^\dagger). \quad (6.12)$$

It is now straightforward to explicitly write the Hamiltonian describing the quadratic interaction, $H_{\text{int},2}$, by inserting the definition of the vector potential (6.2) into Eq. (6.7). This gives

$$H_{\text{int},2} = \frac{e^2}{m} \sum_{j,k,\alpha,\beta} \xi_\alpha \xi_\beta d_j^\dagger d_k \int \phi_j^*(\vec{x}) \left(b_\alpha e^{i\vec{k}_\alpha \cdot \vec{x}} + b_\alpha^\dagger e^{-i\vec{k}_\alpha \cdot \vec{x}} \right) \left(b_\beta e^{i\vec{k}_\beta \cdot \vec{x}} + b_\beta^\dagger e^{-i\vec{k}_\beta \cdot \vec{x}} \right) \phi_k(\vec{x}) d\vec{x}. \quad (6.13)$$

The nonlinear coupling strength can be written as

$$g_{jk\alpha\beta} = \frac{e^2}{2m} \xi_\alpha \xi_\beta \int \phi_j^*(\vec{x}) e^{i(\vec{k}_\alpha + \vec{k}_\beta) \cdot \vec{x}} \phi_k(\vec{x}) d\vec{x}, \quad (6.14)$$

since for every vector \vec{k}_n there exists $\vec{k}_{n'} = -\vec{k}_n$ and thus all the possible combinations of \vec{k} -vectors are handled properly by the sum over both α and β . Let us assume that also the phase of the nonlinear coupling strength can be tuned so that it is real valued. Now the quadratic interaction Hamiltonian takes the following form

$$H_{\text{int},2} = \sum_{j,k,\alpha,\beta} d_j^\dagger d_k g_{jk\alpha\beta} (b_\alpha + b_\alpha^\dagger) (b_\beta + b_\beta^\dagger). \quad (6.15)$$

Two-level systems are now introduced into the model using the electron field operators. A TLS can now be written in terms of Pauli matrices

$$\begin{aligned} \sigma_z &= d_2^\dagger d_2 - d_1^\dagger d_1, \\ \sigma_+ &= \frac{1}{2} (\sigma_x + i\sigma_y) = d_2^\dagger d_1, \\ \sigma_- &= \frac{1}{2} (\sigma_x - i\sigma_y) = d_1^\dagger d_2. \end{aligned} \quad (6.16)$$

These can be applied to the model by letting the summations above to allow only $j, k = 1, 2$. This leads to

$$\begin{aligned} H &= H_{\text{el}} + H_{\text{field}} + H_{\text{int},1} + H_{\text{int},2} \\ &= \frac{\omega_0}{2} \sigma_z + \sum_{\alpha} \omega_{\alpha} b_{\alpha}^{\dagger} b_{\alpha} + \sum_{\alpha} (b_{\alpha} + b_{\alpha}^{\dagger}) (g_{21\alpha} \sigma_+ + g_{12\alpha} \sigma_-) \\ &\quad + \sum_{\alpha,\beta} (b_{\alpha} + b_{\alpha}^{\dagger}) (b_{\beta} + b_{\beta}^{\dagger}) \left[g_{21\alpha\beta} \sigma_+ + g_{12\alpha\beta} \sigma_- \right. \\ &\quad \left. + \frac{1}{2} (g_{22\alpha\beta} - g_{11\alpha\beta}) \sigma_z + \frac{1}{2} (g_{22\alpha\beta} + g_{11\alpha\beta}) \right], \end{aligned} \quad (6.17)$$

where ω_0 is the energy difference between the excited state and the ground state of the TLS.

The above derivation focuses on one mode, but what we are interested in is the tripartite cavity-TLS-environment system. Therefore, I consider now several modes, the fields of the cavity and the bath, with annihilation operators a and c_n , both fields coupling to TLSs. The above calculations can be performed in the case of the vector potential describing both the cavity and the environment modes so that the formulation of Eq. (6.17) for these two fields is

$$\begin{aligned}
H = & \frac{\omega_0}{2}\sigma_z + \omega_{\text{cav}}a^\dagger a + \sum_{\alpha} \omega_{\alpha}c_{\alpha}^{\dagger}c_{\alpha} \\
& + (a + a^\dagger)\left(g_{21a}^c\sigma_+ + g_{12a}^c\sigma_-\right) + \sum_{\alpha} (c_{\alpha} + c_{\alpha}^{\dagger})\left(g_{21\alpha}^e\sigma_+ + g_{12\alpha}^e\sigma_-\right) \\
& + (a + a^\dagger)^2\left[g_{21aa}^c\sigma_+ + g_{12aa}^c\sigma_- + \frac{1}{2}\left(g_{22aa}^c - g_{11aa}^c\right)\sigma_z + \frac{1}{2}\left(g_{22aa}^c + g_{11aa}^c\right)\right] \\
& + \sum_{\alpha,\beta} (c_{\alpha} + c_{\alpha}^{\dagger})(c_{\beta} + c_{\beta}^{\dagger})\left[g_{21\alpha\beta}^e\sigma_+ + g_{12\alpha\beta}^e\sigma_- \right. \\
& \quad \left. + \frac{1}{2}\left(g_{22\alpha\beta}^e - g_{11\alpha\beta}^e\right)\sigma_z + \frac{1}{2}\left(g_{22\alpha\beta}^e + g_{11\alpha\beta}^e\right)\right] \\
& + \sum_{\alpha} (c_{\alpha} + c_{\alpha}^{\dagger})(a + a^\dagger)\left[g_{21\alpha a}^m\sigma_+ + g_{12\alpha a}^m\sigma_- \right. \\
& \quad \left. + \frac{1}{2}\left(g_{22\alpha a}^m - g_{11\alpha a}^m\right)\sigma_z + \frac{1}{2}\left(g_{22\alpha a}^m + g_{11\alpha a}^m\right)\right]
\end{aligned} \tag{6.18}$$

Here the coupling constants between the TLS and the environment and between the TLS and the cavity are denoted with superscripts e and c, respectively, and the subscript a stands for the cavity mode. The mixed coupling constant $g_{jk\alpha a}^m$ has a very similar form to the nonlinear coupling strength $g_{jk\alpha\beta}$. The key difference is that $g_{jk\alpha a}^m$ has contributions from both the environment and the cavity, i.e. it describes the coupling strength of the environment coupling to the cavity via the TLS. The form of the coupling is

$$g_{jk\alpha a}^m = \frac{e^2}{2m}\xi_{\alpha}^e\xi_a^c \int \phi_j^*(\vec{x}) e^{i(\vec{k}_{\alpha}^e + \vec{k}_a^c)\cdot\vec{x}} \phi_k(\vec{x}) d\vec{x}. \tag{6.19}$$

Above in Eq. (6.18), we can see that the coupling between the environment and the cavity arises from their interactions with the TLS, since by taking all the coupling constants to zero, all we have left are the noninteracting Hamiltonians of the TLS, the cavity, and the environment. Most notably, the last summation exhibits an explicit cavity-bath coupling. The interactions between the cavity and the environment are schematically represented in Fig. 13. In Sec. 6.2, I construct an effective model of these interactions utilizing the property that the TLS has a large energy separation compared to the energies of the cavity and the environment.

By looking at the Hamiltonian (6.18) from the perspective that focuses on the TLS being the system of interest, leaving the cavity and the environment as noise sources for the TLS, a few similarities shared with the spin-boson model introduced in Chap. 5 can be seen. The cavity and the environment behave as if they are a bosonic heat bath surrounding the qubit and there is a quadratic coupling between the displacement operators of the cavity and the environment and σ_z like in the extended spin-boson model mentioned above. Interestingly enough, this quadratic dephasing mechanism of the qubit is the only dephasing described by this model. However the tunneling terms describing the

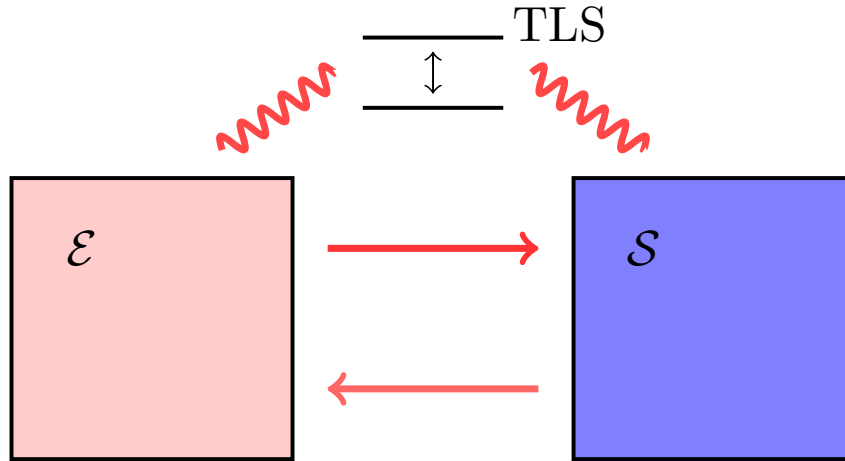


Figure 13: The environment \mathcal{E} and the system \mathcal{S} interact not only directly with each other but also indirectly via a two-level system as given by the Hamiltonian (6.18).

dissipation of the qubit, i.e. the ones proportional to $\sigma_x = \sigma_+ + \sigma_-$, are linearly and quadratically coupled to the displacement operators.

There are interesting special cases of dissipative environments. Recall the definition of symmetrized spectral density, (4.20). Let us consider the symmetrical part of the spectral density of the environment variable $X = \sum_j g_j (c_j + c_j^\dagger)$

$$\bar{S}_{XX}(\omega) = 2J(\omega) \coth\left(\frac{\omega\beta}{2}\right), \quad (6.20)$$

where $\beta = 1/(k_B T)$. $J(\omega)$ is the spectrum of the environment.

A simple dissipation scheme is the *Ohmic dissipation* that requires the environment spectrum to be linearly dependent on frequency, i.e.

$$J(\omega) = \frac{\pi}{2} \alpha \omega \Theta(\omega_{co} - \omega), \quad (6.21)$$

where ω_{co} is a cutoff frequency and the strength of the dissipation is determined by the parameter α . In the high temperature limit, i.e. when $\beta \rightarrow 0$, the dynamics described by the Ohmic dissipation become Markovian [53]. Let us briefly focus on this case. Suppose that the system in focus is a harmonic oscillator described by the Hamiltonian

$$H_S = \frac{p^2}{2m} + \frac{m\omega_{ho}^2}{2} q^2, \quad (6.22)$$

where m , p , q , and ω_{ho} are the mass, momentum, position, and the fundamental frequency of the oscillator. Let the environment be a heat bath whose Hamiltonian is given by (3.9), and let the interaction Hamiltonian between the heat bath and the oscillator be

$$H_I = -qX. \quad (6.23)$$

In the high temperature limit of the Ohmic dissipation model, the Langevin equation for the oscillator can be written as [53]

$$m\ddot{q} = -m\omega_{ho}^2 q - \eta\dot{q} + X_t, \quad (6.24)$$

where X_t is a classical noise term, replacing the quantum mechanical noise X , obeys white noise statistics $\langle X_t X_u \rangle = 2\eta k_B T \delta(t - u)$, and η is the damping ratio. This QLE can then be solved for q .

Another example of different dissipation models is the $1/f$ noise whose symmetrized spectral density

$$\bar{S}_{XX}(\omega) = \frac{E_{1/f}^2}{|\omega|}, \quad (6.25)$$

$E_{1/f}^2 = 2\pi\alpha\omega_s k_B T$, can be derived using *sub-Ohmic* spectrum of the environment

$$J_s(\omega) = \frac{\pi}{2}\alpha\omega_s^{1-s}\omega^s, \quad s < 1, \quad (6.26)$$

in the limit $s \rightarrow 0$. To get the form (6.25) this spectrum can be inserted back to Eq. (6.20) that is approximated to the lowest order in $\omega\beta/2$ at reasonably high temperature.

6.2 Schrieffer–Wolff transformation

The Schrieffer–Wolff transformation allows me to find the effective Hamiltonian on a projection subspace of the overall Hilbert space. The effective Hamiltonian describes the low energy physics on this specific subspace. The following formulation of the theory follows the treatment of Essler et al. [54], and I present the same derivation of the theory for completeness in Appendix C. This theory has been applied to different physical systems, the most prominent arguably being the description of the half-filled Hubbard model in terms of antiferromagnetic Heisenberg model [54].

Consider the stationary Schrödinger equation

$$H|\Psi\rangle = E|\Psi\rangle, \quad (6.27)$$

where H is a Hamiltonian operator acting on Hilbert space \mathcal{H} . Impose now that the Hamiltonian H consists of two parts, pure unperturbed Hamiltonian H_0 with the spectral decomposition

$$H_0 = \sum_n E_n P_n, \quad (6.28)$$

where P_n is a projection operator on a subspace $P_n\mathcal{H}$ of a Hilbert space \mathcal{H} , and a perturbation Hamiltonian H_1 so that

$$H = H_0 + \lambda H_1, \quad (6.29)$$

where the parameter λ , describing the strength of the perturbation, is small.

We rewrite the spectral problem (6.27) as [54]

$$\left[P_n H_1 P_n + \lambda \sum_{m(m \neq n)} \frac{P_n H_1 P_m H_1 P_n}{E_n - E_m} \right] |\phi\rangle = \frac{E - E_n}{\lambda} |\phi\rangle, \quad (6.30)$$

where the effective Hamiltonian on the subspace $P_n\mathcal{H}$ is

$$H_{\text{eff}} = P_n H_1 P_n + \lambda \sum_{m(m \neq n)} \frac{P_n H_1 P_m H_1 P_n}{E_n - E_m} \quad (6.31)$$

and the state $|\phi\rangle \in P_n \mathcal{H}$.

Let us move back to the optical cavity. Let H_0 describe an ensemble of two-level systems, where the energy level separation represents the largest energy scale in the problem, see Fig. 14. The bands formed by the TLSs correspond to the projections P_n . The perturbation Hamiltonian H_1 corresponds to the terms in Eq. (6.18) associated with the dynamics of the cavity and the bath, along with their coupling with the TLSs so that the spin operators σ_{\pm} raise/lower the state between different bands.

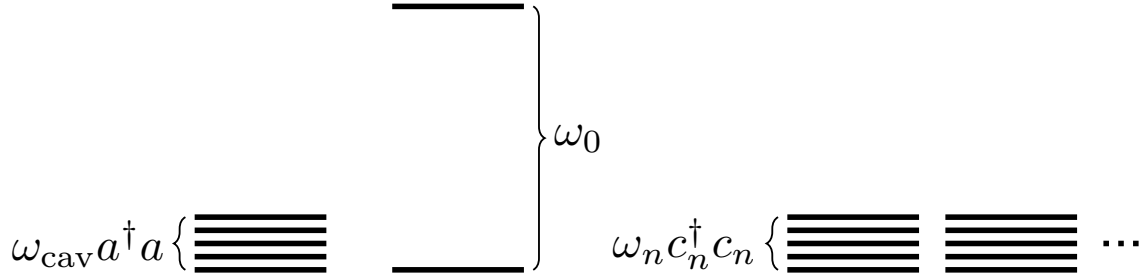


Figure 14: The energy separation ω_0 between the bands of the TLSs is much larger than the energy of the cavity or the environment.

Let us calculate the effective Hamiltonian in parts and start from the first order $P_n H_1 P_n$. Define $\sigma_z |n\rangle = M |n\rangle$, where M is the magnetization quantum number of the state, and $\sigma_{\pm} |n\rangle = |n \pm 1\rangle$. Denote $P_n = |n\rangle \langle n|$. Using these definitions, it can be seen that to the first order only the terms proportional to $\mathbb{1}$ and σ_z remain, since they are diagonal and thus the state $|n\rangle$ is their eigenstate. The other terms cancel out since $\langle n | m \rangle = \delta_{nm}$. The remaining P_n operators are omitted from the following calculations, since the effective Hamiltonian operates on the subspace $P_n \mathcal{H}$. The first order term is

$$\begin{aligned}
P_n H_1 P_n &= \omega_{\text{cav}} a^\dagger a + \sum_{\alpha} \omega_{\alpha} c_{\alpha}^{\dagger} c_{\alpha} \\
&+ \frac{1}{2} (a + a^{\dagger})^2 \left[M (g_{22aa}^c - g_{11aa}^c) + (g_{22aa}^c + g_{11aa}^c) \right] \\
&+ \frac{1}{2} \sum_{\alpha, \beta} (c_{\alpha} + c_{\alpha}^{\dagger}) (c_{\beta} + c_{\beta}^{\dagger}) \left[M (g_{22\alpha\beta}^e - g_{11\alpha\beta}^e) + (g_{22\alpha\beta}^e + g_{11\alpha\beta}^e) \right] \\
&+ \frac{1}{2} \sum_{\alpha} (c_{\alpha} + c_{\alpha}^{\dagger}) (a + a^{\dagger}) \left[M (g_{22\alpha a}^m - g_{11\alpha a}^m) + (g_{22\alpha a}^m + g_{11\alpha a}^m) \right].
\end{aligned} \tag{6.32}$$

Recall the coupling constants, denoted by g , from Eqs. (6.11), (6.14) and (6.19). H_1 contains only operators that raise or lower the state by one or do not affect the state. The latter operators are ruled out by the summation of the second order term of the effective Hamiltonian. Thus the rest of H_{eff} can be written in terms of $P_n H_1 P_{n\pm 1} H_1 P_n$ which are very similar to each other, the only difference being that all the indices 1 and 2 are reversed.

Let us calculate $P_n H_1 P_{n+1} H_1 P_n$ explicitly

$$\begin{aligned}
P_n H_1 P_{n+1} H_1 P_n = & \left[(a + a^\dagger) g_{12a}^c + (a + a^\dagger)^2 g_{12aa}^c + \sum_{\alpha} (c_{\alpha} + c_{\alpha}^\dagger) g_{12\alpha}^e \right. \\
& + \sum_{\alpha, \beta} (c_{\alpha} + c_{\alpha}^\dagger) (c_{\beta} + c_{\beta}^\dagger) g_{12\alpha\beta}^e + \sum_{\alpha} (c_{\alpha} + c_{\alpha}^\dagger) (a + a^\dagger) g_{12\alpha a}^m \left. \right] \\
& \times \left[(a + a^\dagger) g_{21a}^c + (a + a^\dagger)^2 g_{21aa}^c + \sum_{\delta} (c_{\delta} + c_{\delta}^\dagger) g_{21\delta}^e \right. \\
& \left. + \sum_{\delta, \epsilon} (c_{\delta} + c_{\delta}^\dagger) (c_{\epsilon} + c_{\epsilon}^\dagger) g_{21\delta\epsilon}^e + \sum_{\delta} (c_{\delta} + c_{\delta}^\dagger) (a + a^\dagger) g_{21\delta a}^m \right]. \tag{6.33}
\end{aligned}$$

Some of the terms in Eqs. (6.32) and (6.33) can be discarded as insignificant on the basis of the size of their coupling constants. Remember that Eqs. (6.11), (6.14) and (6.19) give us the following relations

$$\begin{aligned}
g_{jk\alpha}^{c/e} & \propto \frac{1}{\sqrt{\omega_{\alpha}^{c/e} V^{c/e}}}, \\
g_{jk\alpha\beta}^{c/e} & \propto \frac{1}{\sqrt{\omega_{\alpha}^{c/e} \omega_{\beta}^{c/e} V^{c/e}}}, \\
g_{jk\alpha a}^m & \propto \frac{1}{\sqrt{\omega_{\alpha}^e \omega_{\text{cav}} V^e V^c}}. \tag{6.34}
\end{aligned}$$

Let us first take a look at the terms $(a + a^\dagger) (c_{\alpha} + c_{\alpha}^\dagger)$ and $(a + a^\dagger)^2 (c_{\alpha} + c_{\alpha}^\dagger)$ since they are the crucial interaction terms in the total Hamiltonian (4.2) where $H_S = \omega_{\text{cav}} a^\dagger a$. With the help of Eqs. (6.32)–(6.34) it can be seen that the strengths of these contributions are proportional to $(\omega_{\text{cav}} \omega_{\alpha}^e V^c V^e)^{-1/2}$ and $(\omega_{\alpha}^e V^e)^{-1/2} (\omega_{\text{cav}} V^c)^{-1}$, respectively.

The cavity is considered to operate in the optical frequency range spanning roughly 400–800 THz, and the environment has a significantly larger volume compared to the volume of the cavity. The separation of the mirrors of an optical cavity is usually in the range from 10^{-5} m to 10^{-2} m [11] making the volume of the cavity small. Therefore any coupling constant connected to fourth order terms in c and/or a is negligible compared to the strengths of the two interaction terms discussed above. These fourth order terms are therefore discarded.

The argument for discarding the other terms that are not linear in the environment degrees of freedom is slightly different. For instance, in order to discard the $(c_{\alpha} + c_{\alpha}^\dagger)^2$ term, it is required that

$$\frac{1}{\omega_{\alpha}^e V^e} \ll \frac{1}{\sqrt{\omega_{\alpha}^e V^e}} \frac{1}{\omega_{\text{cav}} V^c} \Rightarrow \frac{1}{\sqrt{\omega_{\alpha}^e V^e}} \ll \frac{1}{\omega_{\text{cav}} V^c}. \tag{6.35}$$

This inequality is satisfied since the volume of the environment effectively means the volume of the rest of the “universe” outside the cavity, and the volume of the optical cavity is very tiny. Additionally, the frequencies of the environment modes coupling to the cavity are of the same order as the intrinsic frequency of the cavity, making the omission of the $(c_{\alpha} + c_{\alpha}^\dagger)^2$ term justified based on the enormous volume difference of these

two entities. From this follows directly that only terms linear in the environment degrees of freedom are significant.

The volume arguments can be heuristically interpreted as a statement of the locality of the interaction between the cavity and the environment. The cavity is very small, thus it has a large overlap with the TLSs resulting in a strong interaction, whereas the environment modes are more spread out.

In total, I am left with

$$\begin{aligned}
H_{\text{eff}} &= \omega_{\text{cav}} a^\dagger a + \sum_{\alpha} \omega_{\alpha} c_{\alpha}^{\dagger} c_{\alpha} \\
&+ \frac{1}{2} \left[(M+1) g_{22aa}^c + (-M+1) g_{11aa}^c + 2h_{\lambda,n} g_{12a}^c g_{21a}^c \right] (a + a^\dagger)^2 \\
&+ \frac{1}{2} \sum_{\alpha} \left[(M+1) g_{22\alpha a}^m + (-M+1) g_{11\alpha a}^m \right] (c_{\alpha} + c_{\alpha}^{\dagger}) (a + a^\dagger) \\
&+ h_{\lambda,n} \sum_{\alpha} \left[g_{12a}^c g_{21\alpha}^e + g_{21a}^c g_{12\alpha}^e \right] (c_{\alpha} + c_{\alpha}^{\dagger}) (a + a^\dagger) \\
&+ h_{\lambda,n} \left[g_{12a}^c g_{21aa}^c + g_{21a}^c g_{12aa}^c \right] (a + a^\dagger)^3 \\
&+ h_{\lambda,n} \sum_{\alpha} \left[g_{12a}^c g_{21\alpha a}^m + g_{21a}^c g_{12\alpha a}^m + g_{12aa}^c g_{21\alpha}^e + g_{21aa}^c g_{12\alpha}^e \right] \\
&\quad \times (c_{\alpha} + c_{\alpha}^{\dagger}) (a + a^\dagger)^2,
\end{aligned} \tag{6.36}$$

where $h_{\lambda,n} = \lambda / (E_n - E_{n+1}) + \lambda / (E_n - E_{n-1})$.

Defining the following coupling strengths

$$\begin{aligned}
g_2^c &= \frac{1}{2} \left[(M+1) g_{22aa}^c + (-M+1) g_{11aa}^c + 2h_{\lambda,n} g_{12a}^c g_{21a}^c \right], \\
g_3^c &= h_{\lambda,n} \left[g_{12a}^c g_{21aa}^c + g_{21a}^c g_{12aa}^c \right], \\
g_{1,\alpha}^m &= \frac{1}{2} \left[(M+1) g_{22\alpha a}^m + (-M+1) g_{11\alpha a}^m \right] + h_{\lambda,n} \left[g_{12a}^c g_{21\alpha}^e + g_{21a}^c g_{12\alpha}^e \right], \\
g_{2,\alpha}^m &= h_{\lambda,n} \left[g_{12a}^c g_{21\alpha a}^m + g_{21a}^c g_{12\alpha a}^m + g_{12aa}^c g_{21\alpha}^e + g_{21aa}^c g_{12\alpha}^e \right],
\end{aligned} \tag{6.37}$$

and rearranging Eq. (6.36) using the common bosonic commutation relations, one gets

$$\begin{aligned}
H_{\text{eff}} &= (\omega_{\text{cav}} + 2g_2^c) a^\dagger a + \sum_{\alpha} \omega_{\alpha} c_{\alpha}^{\dagger} c_{\alpha} \\
&+ \sum_{\alpha} g_{1,\alpha}^m (c_{\alpha} + c_{\alpha}^{\dagger}) (a + a^\dagger) + \sum_{\alpha} g_{2,\alpha}^m (c_{\alpha} + c_{\alpha}^{\dagger}) (a + a^\dagger)^2 \\
&+ g_2^c (a^2 + a^{\dagger 2} + 1) + g_3^c (3a + a^\dagger + a^3 + a^{\dagger 3} + 3a^\dagger a^2 + 3a^{\dagger 2} a).
\end{aligned} \tag{6.38}$$

This formulation of the effective Hamiltonian justifies the appearance of different linear and nonlinear dynamics of the cavity-environment system when mediated by two-level systems. Most notably the displacement operator of the environment is coupled to the displacement operator of the cavity both linearly and quadratically like the model Hamiltonian introduced in Chap. 4.

Assuming that $(\omega_{\text{cav}} V^c)^{\frac{1}{2}}$ is very small, one can see that the linear coupling $g_{1,\alpha}^m$ is stronger than the quadratic one $g_{2,\alpha}^m$, as it is reasonable to expect. In the numerical calculations above, the linear coupling is considered to be at least three orders of magnitude stronger. Similarly one can justify that the shift of the resonant frequency of the cavity by $2g_2^c$ is negligible compared to the fundamental frequency ω_{cav} .

Additionally parametric coupling terms emerge. Parametric terms a^2 and $a^{\dagger 2}$, causing the cavity field and the pump to have a different phases, are used by Pirkkalainen et al. [55] to better align the theoretical model with the measurement data in their experiment of squeezing the noise of a micromechanical resonator. They also suspect that nonlinear dissipation could be the reason for the appearance of these terms. The above argument of $(\omega_{\text{cav}} V^c)^{\frac{1}{2}}$ being small also means that the second order parametric terms a^2 and $a^{\dagger 2}$ are more significant compared to the third order ones. The first order terms can be omitted by applying a displacement operator on the effective Hamiltonian.

Conclusions

The addition of even a very simple nonlinear coupling between a cavity and its environment alters the behaviour of the cavity distinctly. In the model explored in Chap. 4, the average population of the cavity grows noticeably faster as the function of the strength of the input field up to a certain threshold, after which it starts to decrease due to the nonlinear dissipation mechanism. Moreover multiple equilibrium solutions of the average cavity field emerge for strong enough laser pumping.

In addition, the nonlinear coupling to the environment gives rise to a change to the first-order fluctuations around the equilibrium solution of the cavity field. As a direct result the cavity spectral density is affected. An increased strength of the nonlinear coupling increases the response while decreasing the linewidth. As opposed to the linear model, the phase of the average cavity field also affects the spectral density of the cavity.

As the model discussed above is also applicable to mechanical resonators, these findings emphasize the wealth of the phenomena that potentially can be observed in presence of nonlinear dissipation effects.

References

- [1] J. Kepler. *De Cometis Libelli Tres*. 1619.
- [2] I. Newton. *Opticks*. 1704.
- [3] J.C. Maxwell. *A treatise of electricity and magnetism*. Oxford University Press, 2nd edition, 1881.
- [4] A. Einstein. On the development of our views concerning the nature and constitution of radiation. In *Collected papers of Albert Einstein - Volume 2: The Swiss Years: Writings, 1900-1909 (English translation supplement)*. Princeton University Press, 1989.
- [5] E.F. Nichols and G.F. Hull. The pressure due to radiation. *Astrophysical Journal*, 17:315, 1901.
- [6] P. Lebedev. Untersuchungen über die Druckkräfte des Lichtes. *Annalen der Physik*, 1901.
- [7] A. Ashkin. Trapping of atoms by resonance radiation pressure. *Phys. Rev. Lett.*, 40(12), 1978.
- [8] T.W. Hänsch and A.L. Schawlow. Cooling of gases by laser radiation. *Opt. Commun.*, 13(1), 1975.
- [9] S. Chu. Cold atoms and quantum control. *Nature*, 416, 2002.
- [10] B.P. Abbott et al. Observation of gravitational waves from a binary black hole merger. *Phys. Rev. Lett.*, 116(6), 2016.
- [11] M. Aspelmeyer, T.J. Kippenberg, and F. Marquardt. Cavity optomechanics. *Rev. Mod. Phys.*, 86, 2014.
- [12] Qian J., A.A. Clerk, K. Hammerer, and F. Marquardt. Quantum signatures of the optomechanical instability. *Phys. Rev. Lett.*, 109(253601), 2012.
- [13] A.A. Clerk, M.H. Devoret, S.M. Girvin, F. Marquardt, and R.J. Schoelkopf. Introduction to quantum noise, measurement, and amplification. *Rev. Mod. Phys.*, 82, 2010.
- [14] G.D. Cole and M. Aspelmeyer. Cavity optomechanics: Mechanical memory sees the light. *Nature Nanotechnology*, 6:690, 2011.
- [15] G. Stefanucci and R. van Leeuwen. *Nonequilibrium many-body theory of quantum systems – A modern introduction*. Cambridge University Press, 2013.

- [16] M.E. Peskin and D.V. Schroeder. *An introduction to quantum field theory*. Westview Press, 1995.
- [17] D. Cohen. Chaos, dissipation and quantal Brownian motion. *arXiv:chaodyn/9909024v2*, 15 Aug 2000.
- [18] S.R. de Groot and P. Mazur. *Non-equilibrium thermodynamics*. Dover Publications, 2011.
- [19] H.M. Wiseman and G.J. Milburn. *Quantum measurement and control*. Cambridge University Press, 2009.
- [20] A. Eichler, J. Moser, J. Chaste, M. Zdrojek, I. Wilson-Rae, and A. Bachtold. Non-linear damping in mechanical resonators made from carbon nanotubes and graphene. *Nature Nanotechnology*, 6, 2011.
- [21] A.N. Cleland. *Foundations of nanomechanics*. Springer, Berlin, 2003.
- [22] L.D. Landau and E.M. Lifshitz. *Mechanics*. Pergamon Press Ltd., 2nd edition, 1969.
- [23] S. Zaitsev, O. Shtempluck, E. Buks, and O. Gottlieb. Nonlinear damping in a micro-mechanical oscillator. *arXiv:0911.0833v2 [cond-mat.other]*, 12 Nov 2009.
- [24] S.M. Girvin. *Circuit QED: Superconducting Qubits Coupled to Microwave Photons*. Oxford University Press, 2011.
- [25] M.H. Devoret. Quantum fluctuations in electrical circuits. In S. Reynaud, E. Giacobino, and J. Zinn-Justin, editors, *Fluctuations Quantiques / Quantum Fluctuations: Les Houches Session LXIII, June 27 - July 28, 1995*, page 351. Elsevier, Amsterdam, 1997.
- [26] H.-P. Breuer, E.-M. Laine, J. Piilo, and B. Vacchini. Colloquium: Non-Markovian dynamics in open quantum systems. *Rev. Mod. Phys.*, 88, 2016.
- [27] C.W. Gardiner and M.J. Collett. Input and output in damped quantum systems: Quantum stochastic differential equations and the master equation. *Phys. Rev. A*, 31(6), 1984.
- [28] R. Khan, F. Massel, and T.T. Heikkilä. Cross-Kerr nonlinearity in optomechanical systems. *Phys. Rev. A*, 91(043822), 2015.
- [29] K. Rojan, R. Kraus, T. Fogarty, H. Habibian, A. Minguzzi, and G. Morigi. Localization transition in presence of cavity backaction. *arXiv:1605.01226v1 [quant-ph]*, 4 May 2016.
- [30] F. Marquardt, A.A. Clerk, and S.M. Girvin. Quantum theory of optomechanical cooling. *arXiv:0803.1164v1 [quant-ph]*, 7 Mar 2008.
- [31] M. Le Bellac, F. Mortessagne, and G.G. Batrouni. *Equilibrium and non-equilibrium statistical thermodynamics*. Cambridge University Press, New York, 2004.
- [32] J.C. Sankey, C. Yang, B.M. Swickl, A.M. Jayich, and J.G.E. Harris. Strong and tunable nonlinear optomechanical coupling in a low-loss system. *Nature Physics*, 6:707, 2010.
- [33] J. Preskill. *Lecture Notes for Ph219/CS219: Quantum Information*. California Institute of Technology, 2015.

- [34] D.J. Griffiths. *Introduction to quantum mechanics*. Pearson Education, 2nd edition, 2004.
- [35] B.H. Bransden and C.J. Joachain. *Quantum Mechanics*. Pearson Education Ltd, 2nd edition, 2000.
- [36] D.F. Walls and G.J. Milburn. *Quantum optics*. Springer, 2nd edition, 2010.
- [37] X. Song, M. Oksanen, M.A. Sillanpää, H.G. Craighead, J.M. Parpia, and P.J. Hakonen. Stamp transferred suspended graphene mechanical resonators for radio frequency electrical readout. *Nano Letters*, 12, 2012.
- [38] G.A. Brawley, M.R. Vanner, P.E. Larsen, S. Schmid, A. Boisen, and W.P. Bowen. Nonlinear optomechanical measurement of mechanical motion. *Nature Communications*, 7(10988), 2016.
- [39] V. Singh, O. Shevchuk, Y.M. Blanter, and G.A. Steele. Negative nonlinear damping of a graphene mechanical resonator. *arXiv:1508.04298v1 [cond-mat.mes-hall]*, 18 Aug 2008.
- [40] V. Singh, S.J. Bosman, B.H. Schneider, Y.M. Blanter, A. Castellanos-Gomez, and G.A. Steele. Optomechanical coupling between a multilayer graphene mechanical resonator and a superconducting microwave cavity. *Nature Nanotechnology*, 9, 2014.
- [41] M.R. Hush, I. Lesanovsky, and J.P. Garrahan. A generic map from non-Lindblad to Lindblad master equations. *arXiv:1311.7394v2 [quant-ph]*, 23 Feb 2015.
- [42] A.P. Paz, I.V. Lebedeva, I.V. Tokatly, and A. Rubio. Identification of structural motifs as tunneling two-level systems in amorphous alumina at low temperatures. *Phys. Rev. B*, 90(224202), 2014.
- [43] W.A. Phillips. Two-level states in glasses. *Rep. Prog. Phys.*, 50:1657–1708, 1987.
- [44] J.M. Buriak. Organometallic chemistry on silicon and germanium surfaces. *Chemical Reviews*, 102(5), 2002.
- [45] Z. Shaterzadeh-Yazdi, L. Livadaru, M. Taucer, J. Mutus, J. Pitters, R.A. Wolkov, and B.C. Sanders. Characterizing the rate and coherence of single-electron tunneling between two dangling bonds on the surface of silicon. *arXiv:1305.6359v2 [cond-mat.mes-hall]*, 28 Jan 2014.
- [46] T. Faust, J. Rieger, M.J. Seitner, J.P. Kotthaus, and E.M. Weig. Coherent control of a nanomechanical two-level system. *arXiv:1212.3172v1 [cond-mat.mes-hall]*, 13 Dec 2012.
- [47] F. Mandl. *Quantum mechanics*. Wiley, 1st edition, 1992.
- [48] J.M. Martinis, K.B. Cooper, R. McDermott, M. Steffen, M. Ansmann, K.D Osborn, K. Cicak, S. Oh, D.P. Pappas, R.W. Simmonds, and C.C. Yu. Decoherence in Josephson qubits from dielectric loss. *Phys. Rev. Lett.*, 95(210503), 2005.
- [49] A.D. O’Connell, M. Ansmann, R.C. Bialczak, M. Hofheinz, N. Katz, E. Lucero, C. McKenney, M. Neeley, H. Wang, E.M. Weig, A.N. Cleland, and J.M. Martinis. Microwave dielectric loss at single photon energies and millikelvin temperatures. *Appl. Phys. Lett.*, 92(112903), 2008.

-
- [50] S. Hunklinger and M.v. Schickfus. Acoustic and dielectric properties of glasses at low temperatures. In W.A. Phillips, editor, *Amorphous solids – Low-temperature properties*, chapter 6, page 81. Springer-Verlag Berlin, Heidelberg New York, 1981.
- [51] A.J. Leggett, S. Chakravarty, A.T. Dorsey, M.P.A. Fisher, A. Garg, and W. Zwerger. Dynamics of the dissipative two-state systems. *Rev. Mod. Phys.*, 59(1), 1987.
- [52] A. Shnirman, Y. Makhlin, and G. Schön. Noise and decoherence in quantum two-level systems. *arXiv:cond-mat/0202518v1 [cond-mat.mes-hall]*, 28 Feb 2002.
- [53] L. Diósi. Ohmic vs Markovian heat bath – two-page tutorial. 2012.
- [54] F.H.L Essler, H. Frahm, F. Göhmann, A. Klümper, and V.E. Korepin. *The one-dimensional Hubbard model*. Cambridge University Press, New York, 1st edition, 2005.
- [55] J.M. Pirkkalainen, E. Damskägg, M. Brandt, F. Massel, and M.A. Sillanpää. Squeezing of quantum noise of motion in a micromechanical resonator. *Phys. Rev. Lett.*, 115(243601), 2015.

A

Derivation of the QLE for the nonlinear model Hamiltonian

Let us explicitly express the derivation of the QLE of the system with the nonlinear coupling to the environment (4.1) presented in Sec. 4.1. Consider a total Hamiltonian including the Hamiltonians of the system, the environment, and the interaction between these two

$$\begin{aligned}
 H &= H_S + H_E + H_I \\
 &= H_S + \sum_n \omega_n c_n^\dagger(t) c_n(t) \\
 &\quad + i \sum_n g_n^L [c_n^\dagger(t) a(t) - c_n(t) a^\dagger(t)] + i \sum_n g_n^N [c_n^\dagger(t) a^2(t) - c_n(t) (a^\dagger(t))^2],
 \end{aligned} \tag{A.1}$$

where the operators a and c_n correspond to the system and the environment, respectively, and $g_n^{L(N)}$ is the coupling constant of the (non)linear interaction. The time arguments of the operators are important in the derivation, so they are left explicitly visible.

The system, the environment, and their mutual interaction form a closed system that is subject to unitary time evolution described by the Heisenberg equation of motion (3.7). Since the system Hamiltonian does not have any dependence on the environment field operators c_n , the Heisenberg EOM of the n th environment mode is

$$\dot{c}_n(t) = i[H, c_n(t)] = -i\omega_n c_n(t) + g_n^L a(t) + g_n^N a^2(t). \tag{A.2}$$

This is an ordinary first order linear differential equation that can be solved for a given initial condition $c_n(t_0)$ at $t_0 < t$ to get

$$c_n(t) = e^{-i\omega_n(t-t_0)} c_n(t_0) + g_n^L \int_{t_0}^t e^{-i\omega_n(t-t')} a(t') dt' + g_n^N \int_{t_0}^t e^{-i\omega_n(t-t')} a^2(t') dt'. \tag{A.3}$$

For the system field operator, the Heisenberg EOM gives

$$\dot{a}(t) = i[H, a(t)] = i[H_S, a(t)] - \sum_n (g_n^L + 2g_n^N a^\dagger(t)) c_n(t) \tag{A.4}$$

following from the fact that the Hamiltonian of the environment (3.9) does not depend on the system variable.

The formal solution of c_n (A.3) can now be inserted to the EOM for a to make it a closed

expression in terms of a and a^\dagger

$$\begin{aligned} \dot{a}(t) &= i[H_S, a(t)] - \sum_n (g_n^L + 2g_n^N a^\dagger(t)) e^{-i\omega_n(t-t_0)} c_n(t_0) \\ &\quad - \sum_n (g_n^L + 2g_n^N a^\dagger(t)) \sqrt{\kappa_L} \int_{t_0}^t e^{-i\omega_n(t-t')} a(t') dt' \\ &\quad - \sum_n (g_n^L + 2g_n^N a^\dagger(t)) \sqrt{\kappa_N} \int_{t_0}^t e^{-i\omega_n(t-t')} a^2(t') dt'. \end{aligned} \quad (\text{A.5})$$

Let us assume that the coupling constants g_n^L and g_n^N are independent of frequency

$$(g_n^L)^2 = \frac{\kappa_L}{2\pi D}; \quad (g_n^N)^2 = \frac{\kappa_N}{2\pi D}, \quad (\text{A.6})$$

where D is the density of states over the oscillatory modes and it is constant since the modes are considered to be evenly distributed, i.e. $n = \omega_n D = n \partial n / \partial \omega_n$. With these new definitions, Eq. (A.5) takes the form

$$\begin{aligned} \dot{a}(t) &= i[H_S, a(t)] - \sqrt{\frac{1}{2\pi D}} (\sqrt{\kappa_L} + 2\sqrt{\kappa_N} a^\dagger(t)) \sum_n e^{-i\omega_n(t-t_0)} c_n(t_0) \\ &\quad - \frac{1}{2\pi D} (\sqrt{\kappa_L} + 2\sqrt{\kappa_N} a^\dagger(t)) \sqrt{\kappa_L} \int_{t_0}^t \sum_n e^{-i\omega_n(t-t')} a(t') dt' \\ &\quad - \frac{1}{2\pi D} (\sqrt{\kappa_L} + 2\sqrt{\kappa_N} a^\dagger(t)) \sqrt{\kappa_N} \int_{t_0}^t \sum_n e^{-i\omega_n(t-t')} a^2(t') dt'. \end{aligned} \quad (\text{A.7})$$

Using the definition of the density of states, the following identity of the delta function can be established

$$\sum_n e^{-i\omega_n(t-t')} = \sum_n e^{-i\frac{n}{D}(t-t')} = 2\pi \delta\left(\frac{1}{D}(t-t')\right) = 2\pi |D| \delta(t-t') \quad (\text{A.8})$$

that can be used to formally calculate the integrals of (A.7).

The input field is defined as

$$a_{\text{in}}(t) = -\sqrt{\frac{1}{2\pi D}} \sum_n e^{-i\omega_n(t-t_0)} c_n(t_0). \quad (\text{A.9})$$

I use Eqs. (A.8) and (A.9) on Eq. (A.7) to get the QLE of a

$$\begin{aligned} \dot{a}(t) &= i[H_S, a(t)] - \frac{\kappa_L}{2} a(t) - \kappa_N a^\dagger(t) a^2(t) - \sqrt{\kappa_L \kappa_N} \left(a^\dagger(t) a(t) + \frac{1}{2} a^2(t) \right) \\ &\quad + \sqrt{\kappa_L} a_{\text{in}}(t) + 2\sqrt{\kappa_N} a^\dagger(t) a_{\text{in}}(t). \end{aligned} \quad (\text{A.10})$$

B

Derivation of the metastable–stable threshold value

Consider the zeroth order approximation in fluctuations of the QLE (4.11) of the nonlinearly dissipative harmonic oscillator.

$$0 = i\Delta\alpha_t - \frac{\kappa_L}{2}\alpha_t - \kappa_N\alpha_t^*\alpha_t^2 - \sqrt{\kappa_L\kappa_N}\left(|\alpha|^2 + \frac{1}{2}\alpha_t^2\right) + \sqrt{\kappa_L}\alpha_{\text{in}} + 2\sqrt{\kappa_N}\alpha_t^*\alpha_{\text{in}}, \quad (\text{B.1})$$

where $\Delta = \omega_p - \omega_{\text{cav}}$ is the detuning of the cavity. Divide the approximated EOM to its real and imaginary parts. I denote $\text{Re}(\alpha_t) = x$ and $\text{Im}(\alpha_t) = y$. In the following, I assume that α_{in} is a real number.

$$\begin{cases} 0 = -\Delta y - \frac{\kappa_L}{2}x - \kappa_N(x^3 + xy^2) - \sqrt{\kappa_L\kappa_N}\left(\frac{3}{2}x + \frac{1}{2}y\right) + \sqrt{\kappa_L}\alpha_{\text{in}} + 2\sqrt{\kappa_N}x\alpha_{\text{in}} \\ 0 = \Delta x - \frac{\kappa_L}{2}y - \kappa_N(x^2y + y^3) - \sqrt{\kappa_L\kappa_N}xy - 2\sqrt{\kappa_N}y\alpha_{\text{in}} \end{cases} \quad (\text{B.2})$$

For large enough values of the input field, this pair of equations has multiple solutions of $|\alpha|$, as seen in Fig. 7. The smallest valued one of these corresponds to the lowest population of the oscillator, thus making it the stable solution. In the following, I derive an expression of the threshold value of the input field where one of the metastable solutions becomes the stable one. Unfortunately EOM (B.2) is too convoluted for this threshold to be solved analytically exactly. Therefore I take the lowest order approximation in κ_N in the limit $\kappa_L \gg \kappa_N$

$$\begin{cases} 0 = -\Delta y - \frac{\kappa_L}{2}x - \sqrt{\kappa_L\kappa_N}\left(\frac{3}{2}x + \frac{1}{2}y\right) + \sqrt{\kappa_L}\alpha_{\text{in}} + 2\sqrt{\kappa_N}x\alpha_{\text{in}} \\ 0 = \Delta x - \frac{\kappa_L}{2}y - \sqrt{\kappa_L\kappa_N}xy - 2\sqrt{\kappa_N}y\alpha_{\text{in}}. \end{cases} \quad (\text{B.3})$$

This pair of equations can be thought as a representation of two conic shapes, whose intersections I am interested in. The problem is however a bit more subtle since I am after the value of the input field where two solutions of $|\alpha|$ intersect, i.e. the intersections of the two conics need to be of equivalent distance from the origin. Even this relatively simple form does not produce any meaningful analytical expression of the threshold. Therefore further approximations are needed. I solve formally for y to get

$$y = \frac{\Delta x}{\frac{\kappa_L}{2} + 2\sqrt{\kappa_N}\alpha_{\text{in}} + \sqrt{\kappa_L\kappa_N}x}, \quad (\text{B.4})$$

and I take the lowest, the first, order approximation of this with respect to x granting me

$$y = \frac{\Delta x}{\frac{\kappa_L}{2} + 2\sqrt{\kappa_N}\alpha_{\text{in}}}. \quad (\text{B.5})$$

This approximation is valid when $2\alpha_{\text{in}} \gg \sqrt{\kappa_L}x$, i.e. when

$$|\alpha|^2 \ll \frac{4\alpha_{\text{in}}^2}{\kappa_L}. \quad (\text{B.6})$$

Looking at the steady state solution of the linearly coupled cavity, i.e. Eq. (4.13) in the limit $\kappa_N = 0$, one can solve

$$\alpha_t = \frac{\sqrt{\kappa_L}}{\frac{\kappa_L}{2} - i\Delta} \alpha_{\text{in}}. \quad (\text{B.7})$$

This shows that $|\alpha|$ acquires its maximum value in resonance so that

$$|\alpha|^2 = \frac{4\alpha_{\text{in}}^2}{\kappa_L} \quad (\text{B.8})$$

validating the approximation of y (B.5) in the regime $\Delta \gg \kappa_L$. This approximation can be plugged back into Eq. (B.3). Now the pair of equations is easily solvable and the approximate position of the threshold, where a metastable solution becomes the stable one, is

$$\alpha_{\text{in}}^{\text{th}} = \frac{\sqrt{\kappa_L^2 + 4\Delta^2}}{4\sqrt{\kappa_N}}. \quad (\text{B.9})$$

C

Derivation of the Schrieffer–Wolff transformation

Here I present the derivation of the formulation of the Schrieffer–Wolff method used in Sec. 6.2. The derivation follows the presentation by Essler et al. [54].

Let P be a projection operator on a subspace $P\mathcal{H}$ of a Hilbert space \mathcal{H} , and let H be a Hamiltonian acting on this Hilbert space. Define the operator $Q = 1 - P$. The following relations

$$PHP|\Psi\rangle + PHQ|\Psi\rangle = PHP|\Psi\rangle + PH|\Psi\rangle - PHP|\Psi\rangle = PE|\Psi\rangle \quad (\text{C.1a})$$

$$QHP|\Psi\rangle + QHQ|\Psi\rangle = E|\Psi\rangle - EP|\Psi\rangle = EQ|\Psi\rangle \quad (\text{C.1b})$$

are satisfied if and only if the Schrödinger equation

$$H|\Psi\rangle = E|\Psi\rangle \quad (\text{C.2})$$

holds. Rewriting Eq. (C.1b) gives

$$\begin{aligned} EQ|\Psi\rangle - QHQ|\Psi\rangle &= (E - QH)Q|\Psi\rangle = QHP|\Psi\rangle \\ \Rightarrow Q|\Psi\rangle &= (E - QH)^{-1}QHP|\Psi\rangle. \end{aligned} \quad (\text{C.3})$$

This result can be plugged back into Eq. (C.1a) to acquire

$$\begin{aligned} PE|\Psi\rangle &= PHP|\Psi\rangle + PH(E - QH)^{-1}QHP|\Psi\rangle \\ \Rightarrow EP|\Psi\rangle &= PH[1 + (E - QH)^{-1}QH]P|\Psi\rangle. \end{aligned} \quad (\text{C.4})$$

Define now

$$\hat{H}(E) = PH[1 + (E - QH)^{-1}QH], \quad (\text{C.5a})$$

$$|\phi\rangle = P|\Psi\rangle. \quad (\text{C.5b})$$

Consider that the Hamiltonian H consists of two parts, pure unperturbed Hamiltonian H_0 with the spectral decomposition

$$H_0 = \sum_n E_n P_n \quad (\text{C.6})$$

and a perturbation Hamiltonian H_1 so that

$$H = H_0 + \lambda H_1, \quad (\text{C.7})$$

where the parameter λ , describing the strength of the perturbation, is small. Define $\hat{H}_n(E)$ by substituting the projection operator P in the definition of $\hat{H}(E)$, (C.5a), for P_n . Note that all the results derived for the general projection P hold also for P_n .

Using the properties of P_n , Q_n , and H_0 , I can write [54]

$$\hat{H}_n(E) = \left[E_n + P_n H_1 \sum_{k=0}^{\infty} \lambda^{k+1} \left(\sum_{m(m \neq n)} \frac{P_m H_1}{E - E_m} \right)^k \right] P_n. \quad (\text{C.8})$$

By rearranging some terms, Eq. (C.4) can be written as

$$P_n H_1 \sum_{k=0}^{\infty} \lambda^{k+1} \left(\sum_{m(m \neq n)} \frac{P_m H_1}{E - E_m} \right)^k |\phi\rangle = (E - E_n) |\phi\rangle. \quad (\text{C.9})$$

Note that here $|\phi\rangle$ is redefined to be included in $P_n \mathcal{H}$.

When $\lambda = 0$, the exact solution of this problem is $E = E_n$. For a small $\lambda \neq 0$ a perturbative series around this known exact solution can be constructed. Up to the second order it is

$$E = E_n + \lambda E_n^{(1)} + \lambda^2 E_n^{(2)}. \quad (\text{C.10})$$

Now the spectral problem can be written as [54]

$$\left[P_n H_1 P_n + \lambda \sum_{m(m \neq n)} \frac{P_n H_1 P_m H_1 P_n}{E_n - E_m} \right] |\phi\rangle = \frac{E - E_n}{\lambda} |\phi\rangle, \quad (\text{C.11})$$

where the effective Hamiltonian on the subspace $P_n \mathcal{H}$ is

$$H_{\text{eff}} = P_n H_1 P_n + \lambda \sum_{m(m \neq n)} \frac{P_n H_1 P_m H_1 P_n}{E_n - E_m}. \quad (\text{C.12})$$

D

Fourier transform conventions

The Fourier transform conventions used in this work are

$$\begin{aligned} a(t) &= \int_{-\infty}^{\infty} \frac{d\omega}{2\pi} a(\omega) e^{-i\omega t}, \\ a^\dagger(t) &= \int_{-\infty}^{\infty} \frac{d\omega}{2\pi} a^\dagger(-\omega) e^{-i\omega t}, \\ a(\omega) &= \int_{-\infty}^{\infty} dt a(t) e^{i\omega t}, \\ a^\dagger(\omega) &= \int_{-\infty}^{\infty} dt a^\dagger(-t) e^{i\omega t}. \end{aligned} \tag{D.1}$$

Let us show that Fourier transforming a differential equation turns it into an algebraic equation. This happens because the following property of Fourier transform of a derivative. Integration by parts gives us

$$\begin{aligned} \int_{-\infty}^{\infty} dt \dot{a}(t) e^{i\omega t} &= a(t) e^{i\omega t} \Big|_{-\infty}^{\infty} - i\omega \int_{-\infty}^{\infty} dt a(t) e^{i\omega t} = -i\omega \int_{-\infty}^{\infty} dt a(t) e^{i\omega t}, \\ \int_{-\infty}^{\infty} dt \dot{a}^\dagger(t) e^{i\omega t} &= a^\dagger(t) e^{i\omega t} \Big|_{-\infty}^{\infty} - i\omega \int_{-\infty}^{\infty} dt a^\dagger(t) e^{i\omega t} = -i\omega \int_{-\infty}^{\infty} dt a^\dagger(t) e^{i\omega t} \end{aligned} \tag{D.2}$$

The rightmost integrals can be identified using the above definitions of the Fourier transform to show that the Fourier transforms of $\dot{a}(t)$ and $\dot{a}^\dagger(t)$, respectively, give us

$$\begin{aligned} \int_{-\infty}^{\infty} dt \dot{a}(t) e^{i\omega t} &= -i\omega a(\omega), \\ \int_{-\infty}^{\infty} dt \dot{a}^\dagger(t) e^{i\omega t} &= -i\omega a^\dagger(-\omega). \end{aligned} \tag{D.3}$$